Journal of Medicinal Chemistry

Article

Antileishmanial Activity of Pyrazolopyridine Derivatives and their Potential as Adjunct Therapy with Miltefosine

Devireddy Anand, Pawan Kumar Yadav, Om P. S. Patel, Naveen Parmar, Rahul K. Maurya, Preeti Vishwakarma, Kanumuri S. R. Raju, Isha Taneja, Muhammad Wahajuddin, Susanta Kar, and Prem P. Yadav

J. Med. Chem., **Just Accepted Manuscript** • DOI: 10.1021/acs.jmedchem.6b01447 • Publication Date (Web): 06 Jan 2017

ACS Publications

Journal of Medicinal Chemistry is published by the American Chemical Society. 1155 Sixteenth Street N.W., Washington, DC 20036

Antileishmanial Activity of Pyrazolopyridine Derivatives and their Potential as Adjunct Therapy with Miltefosine

Devireddy Anand,[†,#] Pawan Kumar Yadav,[‡,#,⊥] Om P. S. Patel,[†] Naveen Parmar,[‡,⊥] Rahul K. Maurya,[†] Preeti Vishwakarma,[‡,⊥] Kanumuri S. R. Raju,[§,⊥] Isha Taneja,[§,⊥] M. Wahajuddin,[§,⊥] Susanta Kar,[*,‡,⊥] and Prem P. Yadav[*,†,⊥]

[†]Medicinal and Process Chemistry Division, CSIR-Central Drug Research Institute, BS-10/1, Sector 10, Jankipuram Extension, Sitapur Road, Lucknow 226031, India.

[‡]Parasitology Division, CSIR-Central Drug Research Institute, BS-10/1, Sector 10, Jankipuram Extension, Sitapur Road, Lucknow 226031, India.

[§]Pharmacokinetics and Metabolism Division, CSIR-Central Drug Research Institute, BS-10/1, Sector 10, Jankipuram Extension, Sitapur Road, Lucknow 226031, India.

[⊥]Academy of Scientific and Innovative Research, Anusandhan Bhawan, New Delhi 110025, India

ABSTRACT. A series of pyrazolo(dihydro)pyridines were synthesized and evaluated for antileishmanial efficacy against experimental visceral leishmaniasis. Among all, compounds **6d** and **6j** exhibited better activity than miltefosine against the intracellular amastigotes. Compound **6j** (50 mg/kg/day) was further studied against *Leishmania donovani*/BALB/c mice via the intraperitoneal route for 5 days and displayed >91 and >93% clearances in splenic and liver parasitic burden, respectively. Combination treatment of **6j** with the sub-curative dose of miltefosine (5 mg/kg) in BALB/c mice almost completely ameliorated the disease (>97% inhibition) by augmenting nitric oxide generation and shifting the immune response towards Th1 mode. Furthermore, investigating the effect of **6j** on Leishmania promastigotes revealed that it induced molecular events like a loss in mitochondrial membrane potential, externalization of phosphatidylserine and DNA fragmentation that ultimately resulted in programmed cell death of the parasite. These results along with pharmacokinetic studies suggested that **6j** could be a promising lead for treating VL as an adjunct therapy with miltefosine.

INTRODUCTION

Leishmaniasis, designated as a neglected tropical disease (NTD) is a chronic infection caused by an obligate intra-macrophage protozoan parasite that belongs to the genus *Leishmania*, and in recent times has developed into a major health problem worldwide.[1] Among all forms of leishmaniasis, visceral leishmaniasis (VL) or kala-azar is the most serious form of the disease. It affects mainly the internal organs like liver, spleen and bone marrow resulting in a lethal condition if left untreated.[2] An estimated 400,000 new cases of VL occurs each year all over the world. Unfortunately, 90% of VL patients are present in just six countries, *viz*., Bangladesh, Brazil, Ethiopia, India, South Sudan and Sudan.[2] It is characterized by irregular bouts of fever, weight loss, enlargement of the liver and spleen, and anemia. The VL is mainly caused by *L. donovani* in the Indian subcontinent and East Africa.[3] In the absence of effective and potential vaccine candidates, chemotherapeutic regimens remain the mainstay of treatment for VL. In the past, pentavalent antimonials (pentostam and glucantime) were recommended as the first line of treatment for VL for more than 60 years, but the emergence of drug-resistant strains of the parasite have limited their use in endemic areas, especially in the Bihar state of India.[4] Therapeutic options for VL have been improved in recent years such as oral drug miltefosine, a variety of liposomal formulations of amphotericin B, aminoglycoside antibiotic paromomycin, and pentamidine. However, major concerns like teratogenicity, nephrotoxicity, hepatotoxicity, long half-life, ototoxicity, parenteral administration for a longer duration, and unaffordable cost are associated with present antileishmanial chemotherapeutic agents.[5] Therefore, there is an urgent need of effective chemotherapeutics with improved pharmacological properties and minimal side effects. Nowadays, combination therapy is one of the alternative approaches to prevent the resistance developed by the parasite to monotherapy regimen, as it also increases the

lifetime of existing drugs and shortens the duration of therapy. The parasite *Leishmania* has established numerous mechanisms by which it inactivates the host protective immune response to successfully survive within macrophages. A further outcome of the disease is regulated by the induction of immunosuppressive molecules that includes transforming growth factor (TGF)-β, interleukin (IL)-10 released by Th2 cell population.[6] These Th2 biasing molecules, in turn, hamper the normal host immune response by inhibiting host-protective microbicidal molecules like interferon-γ (IFN)-γ, IL-12, tumor necrosis factor-α (TNF-α), nitric oxide (NO) and reactive oxygen species (ROS).[6-8] Unfortunately, chemotherapy against VL is observed to be associated with various limitations. Thus the use of established antileishmanial agents at lower doses in combination with novel agents that induced immunostimulation in adjunct with parasite killing will be an effective strategy for the treatment of VL.

According to a recent review on the analysis of FDA approved drugs regarding structural diversity and substitution pattern, the average numbers of nitrogen per drug is 2.5 for all the small molecule drugs.[9] The literature reports on antileishmanial leads revealed that the nitrogen containing heterocycles are very important class of compounds in antileishmanial drug discovery.[3] Roy *et al.,*[10] reported that the di-indolylmethane (DIM) is a potent inhibitor of *L. donovani* topoisomerase I enzyme, it binds strongly to the free enzyme and DIM stabilizes topoisomerase I-DNA cleavage complexes *in vitro* and *in vivo*. Similarly, dihydropyridopyrimidine class of compound exhibited *in vitro* antileishmanial activity in promastigote and amastigote models.[11] Mello and coworkers studied the *in vitro* antileishmanial activity and QSAR properties of 4-anilinopyrazolopyridine-5-carboxylic esters.[12] Kunick *et al*., demonstrated that 2-(3-aryl-3-oxopropenyl)-9-*tert*-butyl-paullones showed activity against both axenic amastigotes and parasites in host macrophages without exhibiting toxicity to human host

cells.[13] Indole-containing benzimidamide was identified as potential antileishmanial compound possessing 10 times better activity and 401-fold less toxicity than the drug pentamidine in cell-based assays.[14] Aminopyrazole ureas and quinazoline class of compounds have been identified as potential antileishmanial agents in a recent report.[15] Based on the frequently encountered antileishmanial scaffolds *i.e.* indole, pyrazole, and pyridine, we designed and synthesized indole appended pyrazolodihydropyridines and pyrazolopyridines as antileishmanial prototypes (Figure 1).

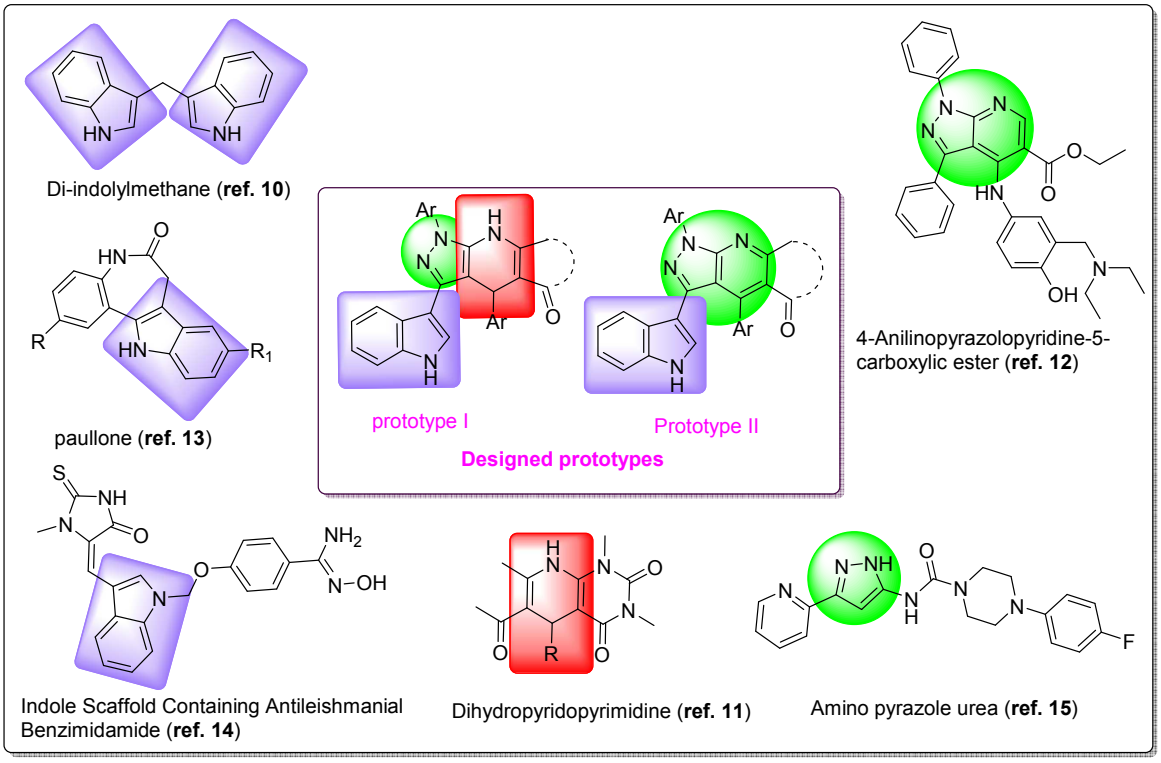

Figure 1. Designing of pyrazolodihydropyridine/pyrazolopyridine hybrids based on reported representative antileishmanial candidates.[10-15]

The designed prototypes can be accessed via multicomponent reaction (MCR)[16] strategy using suitable amine, aldehyde and 1,3-diketone source. MCRs have become a significant area of research in organic and medicinal chemistry due to their atom- and step-economy and formation of structurally diverse scaffolds for biological applications. This integrative nature of MCRs is

attractive when a real need in molecular diversity exists. Herein, we report a MCR approach towards the synthesis of indole appended pyrazolopyridines and pyrazolodihydropyridines and their antileishmanial activity along with combination studies of most potent compound **6j** with miltefosine to achieve better therapeutic value.

RESULTS AND DISCUSSION

Chemistry. Fused pyrazoles are an important scaffold in medicinal chemistry and tremendous efforts have been devoted in the literature to synthesize these molecules.[17] In the present study, pyrazolodihydropyridine and pyrazolopyridine compounds were synthesized as presented in Scheme 1. The synthesis was initiated with the cyanoacetylation of indole **1** by using cyanoacetic acid in acetic anhydride at 60-70 °C by using reported procedure.[18] The 3-cyanoacetyl indole (**2)** thus obtained was further treated with substituted aryl hydrazines in the presence of *p*-toluenesulfonic acid monohydrate (*p*-TsOH.H_2O) as the catalyst in EtOH under reflux conditions to afford the respective 1-aryl-3-indolyl-5-amino pyrazoles **3** in excellent yields of >80%.[19] The reaction of 5-aminopyrazoles **3**, cyclic 1,3-diketones **4** and aryl aldehydes **5** in acetic acid at 100-110 °C afforded the corresponding pyrazolopyridines **7** in good to excellent yields from 68% to 77% as mentioned in the experimental section. In few cases, the pyrazolodihydropyridine derivatives **6** were formed as the major product even after prolonged reaction time. The pyrazolodihydropyridines were further oxidized to aromatized compounds **7** in the presence of 2,3-dichloro-5,6-dicyanobenzoquinone (DDQ) in acetonitrile. It was noteworthy to mention that most of the compounds were purified via crystallization in EtOH, without the need of column chromatography (see; experimental section). All the synthesized compounds were characterized by standard spectroscopic analysis such as ^{1}H, ^{13}C NMR, and ESIHRMS.

Scheme 1. Synthesis of Pyrazolodihydropyridine and Pyrazolopyridine Derivatives[a]

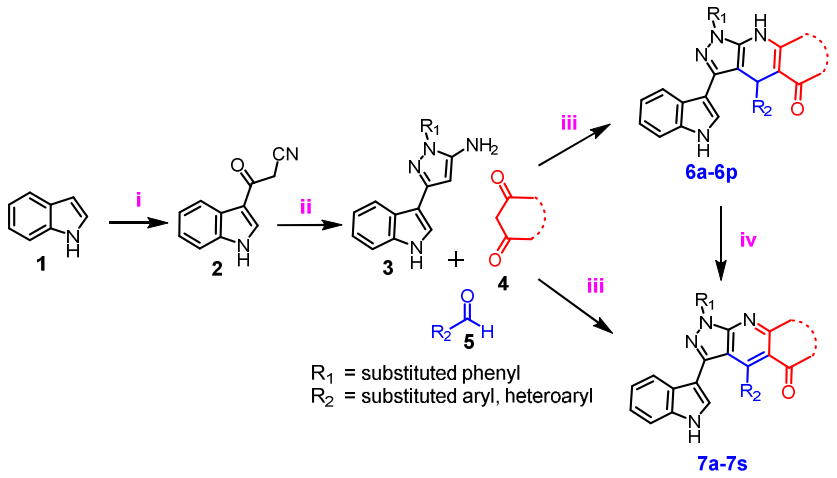

Prototype I	Prototype II
(i) 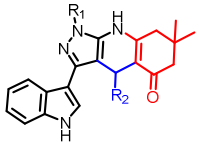	(iv) 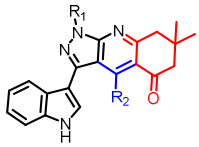
6a; $R_1 = R_2 =$ 4-chlorophenyl **6b:** R_1 = 4-fluorophenyl, R_2 = 4-chlorophenyl **6c;** R_1 = 4-chlorophenyl, R_2 = 3,4,5-trimethoxyphenyl **6d;** R_1 = 3,4-dichlorophenyl, R_2 = 2,5-dimethoxyphenyl **6e;** R_1 = 3,4-dichlorophenyl, R_2 = 3,4-dimethoxyphenyl **6f;** R_1 = 4-chlorophenyl, R_2 = 2-thiophene	**7a;** R_1 = 4-chlorophenyl, R_2 = 2,4-dichlorophenyl **7b;** R_1 = 4-fluorophenyl, R_2 = 2,4-dichlorophenyl **7c;** $R_1 = R_2$ = 4-chlorophenyl **7d;** R_1 = 4-fluorophenyl, R_2 = 4-chlorophenyl **7e;** R_1 = 4-chlorophenyl, R_2 = 4-methoxyphenyl **7f;** R_1 = 4-chlorophenyl, R_2 = 2,5-dimethoxyphenyl **7g;** R_1 = 4-chlorophenyl, R_2 = 2,3,4-trimethoxyphenyl **7h;** R_1 = 4-fluorophenyl, R_2 = 2,5-dimethoxyphenyl **7i;** R_1 = 3,4-dichlorophenyl, R_2 = 3,4-dimethoxyphenyl **7j;** R_1 = 4-chlorophenyl, R_2= 3,4,5-trimethoxyphenyl **7k;** R_1 = 3,4-dichlorophenyl, R_2 = 2,5-dimethoxyphenyl
(ii) 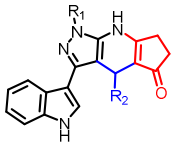	(v) 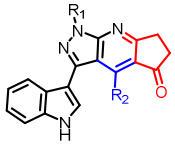
6g; R_1 = 4-chlorophenyl, R_2 = 2,5-dimethoxyphenyl **6h;** R_1 = 4-chlorophenyl, R_2 = 3,4,5-trimethoxyphenyl **6i;** R_1 = 4-chlorophenyl, R_2 = 4-Hydroxy-3,5-dimethoxyphenyl **6j;** R_1 = 3,4-dichlorophenyl, R_2 = 3,4-dimethoxyphenyl **6k;** R_1 = 4-fluorophenyl, R_2 = 4-Hydroxy-3,5-dimethoxyphenyl	**7l;** R_1 = 4-chlorophenyl, R_2 = 2,5-dimethoxyphenyl **7m;** R_1 = 4-chlorophenyl, R_2= 3,4,5-trimethoxyphenyl **7n;** R_1 = 3,4-dichlorophenyl, R_2 = 3,4-dimethoxyphenyl
(iii) 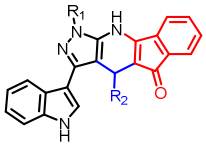	(vi) 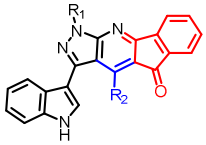
6l; $R_1 = R_2$ = 4-chlorophenyl **6m;** R_1 = 4-fluorophenyl, R_2 = 4-chlorophenyl **6n;** R_1 = 4-chlorophenyl, R_2 = 2,3,4-trimethoxyphenyl **6o;** R_1 = 4-chlorophenyl, R_2 = 2-thiophene	**7o;** R_1 = 4-chlorophenyl, R_2 = 4-methoxyphenyl **7p;** R_1 = 4-chlorophenyl, R_2 = 2,5-dimethoxyphenyl **7q;** R_1 = 4-chlorophenyl, R_2 = 3,4,5-trimethoxyphenyl **7r;** R_1 = 4-fluorophenyl, R_2 = 2,5-dimethoxyphenyl **7s;** R_1 = 4-chlorophenyl,R_2 = 2,3,4-trimethoxyphenyl

[a]Reagents and conditions**. (i)** cyanoacetic acid, Ac_2O, 60-70 °C, 10 min; **(ii)** substituted phenylhydrazines, *p*-TsOH, EtOH, reflux, 2 h; **(iii)** CH_3COOH, 100-110 °C, 2 h; **(iv)** DDQ, acetonitrile, RT, 2 h.

Biological Activity. *In Vitro Antileishmanial Activity of Pyrazolodihydropyridine and Pyrazolopyridine Derivatives.* The antileishmanial activity of pyrazolopyridine derivatives (prototype I and II) was evaluated at 25 and 50 μM concentrations against extracellular promastigotes and intracellular amastigotes of luciferase expressing *L. donovani*. The preliminary results revealed that nine compounds (**6c**, **6d**, **6f-j**, **7h** and **7n**) were found to be active against promastigotes at the concentration of 50 μM with the inhibition rate between 80-95% (Table 1). All the compounds were also examined for their efficacy against amastigote stage of the parasite in *L. donovani* infected J774 macrophages. Among all, the compounds **6d** and **6j** showed excellent activity with parasite killing >95% at 50 μM (Table 1). However, other compounds **6c**, **6f-i**, **7h** **7k** and **7n** exhibit less to moderate activity against intracellular amastigotes stage with inhibition ranging from 28-60% at 50 μM (Table 1). Further, the half maximal inhibition concentrations (IC_{50}) of **6d** and **6j** were found to be 9.59 and 7.19 μM against promastigotes, and 7.36 and 4.05 μM against amastigotes, respectively, which is better than antileishmanial drug miltefosine (antiamastigote IC_{50}: 9.46 μM) (Table 2). Furthermore, the MIC value was calculated by treatment of extracellular promastigotes and intracellular amastigotes with six different concentrations of compounds **6d** and **6j** ranging from 200-6.25 μM by two-fold dilutions. We observed maximum parasite inhibition at a dose of 50 μM for the compounds **6d** and **6j**, which was > 90 and > 95% for promastigotes and amastigotes, respectively. At higher concentration (100 and 200 μM) the percentage inhibition of both promastigotes and amastigotes by **6d** and **6j** did not alter significantly and was almost equal to 50 μM. Therefore, 50 μM doses of both **6d** and **6j** were considered as MIC.

Table 1. *In Vitro* Antileishmanial Activity of Pyrazolodihydropyridines and Pyrazolopyridine Derivatives

entry	promastigotes growth inhibition (%)		amastigotes growth inhibition (%)	
	25 μM	50 μM	25 μM	50 μM
6a	62.5 ± 6.2	65.4 ± 5.3	NSI[a]	NSI
6b	54.3 ± 5.4	65.3 ± 4.3	NSI	NSI
6c	79.3 ± 7.8	86.7 ± 2.8	23.6 ± 2.9	28.2 ± 3.5
6d	**85.9 ± 5.9**	**90.6 ± 3.2**	**91.5 ± 3.5**	**95.8 ± 2.5**
6e	52.3 ± 4.4	59.5 ± 4.3	NSI	NSI
6f	82.5 ± 5.8	86.5 ± 5.6	43.8 ± 3.8	51.7 ± 4.1
6g	85.5 ± 4.3	93.2 ± 5.1	37.3 ± 5.2	42.6 ± 4.5
6h	78.4 ± 6.5	81.2 ± 6.3	45.2 ± 4.3	59.6 ± 5.1
6i	79.1 ± 4.7	89.6 ± 3.2	25.2 ± 2.9	30.7 ± 3.8
6j	**91.7 ± 5.2**	**93.3 ± 3.8**	**96.8 ± 2.2**	**97.3 ± 1.9**
6k	56.5 ± 4.8	66.9 ± 4.9	NSI	NSI
6l	49.1 ± 5.6	62.4 ± 4.8	NSI	NSI
6m	54.2 ± 4.6	68.3 ± 4.7	NSI	NSI
6n	64.2 ± 6.5	67.4 ± 5.2	NSI	NSI
6o	65.3 ± 4.8	69.2 ± 3.9	NSI	NSI
7a	35.7 ± 6.7	40.6 ± 4.8	NSI	NSI
7b	44.6 ± 3.5	48.4 ± 5.3	NSI	NSI
7c	56.7 ± 4.8	67.4 ± 4.3	NSI	NSI
7d	61.3 ± 5.4	68.6 ± 3.6	NSI	NSI
7e	44.3 ± 3.9	52.0 ± 4.3	NSI	NSI
7f	50.7 ± 5.8	69.6 ± 4.9	NSI	NSI
7g	40.2 ± 4.7	54.3 ± 5.2	NSI	NSI
7h	84.1 ± 6.4	90.3 ± 3.8	22.4 ± 3.4	27.9 ± 2.8
7i	59.4 ± 5.8	74.1 ± 5.7	NSI	NSI
7j	59.1 ± 6.3	68.6 ± 6.1	NSI	NSI
7k	41.3 ± 4.9	51.8 ± 4.8	24.6 ± 3.3	41.3 ± 3.8
7l	61.2 ± 6.1	67.2 ± 5.3	NSI	NSI
7m	66.8 ± 5.2	72.3 ± 5.8	NSI	NSI
7n	52.4 ± 3.8	81.1 ± 4.7	20.8 ± 3.3	34.3 ± 3.7
7o	27.5 ± 4.6	33.4 ± 5.2	NSI	NSI
7p	44.6 ± 5.3	53.6 ± 4.8	NSI	NSI
7q	28.3 ± 6.7	41.1 ± 5.3	NSI	NSI
7r	49.8 ± 4.9	58.3 ± 5.1	NSI	NSI
7s	52.6 ± 5.3	63.4 ± 4.7	NSI	NSI
Miltefosine	**100**	**100**	**99.8 ± 0.1**	**100**

[a]NSI (no significant inhibition). Percentage inhibitions are represented as means ± standard deviations for at least three independent experiments for each compound.

Table 2: Half Maximal Concentration (IC_{50}) and Selectivity Index of Compounds **6d** and **6j**

entry	antiamastigote IC_{50} (μM)[a]	cytotoxicity (CC_{50} μM)		selectivity index $SI=CC_{50}/IC_{50}$	
		J774 cells	Vero cells	J774 cells	Vero cells
6d	7.36	482.5	497.6	65.5	67.6
6j	4.05	409.4	438.5	101	108.2
Miltefosine	9.46	55.7	50.8	5.8	5.3

[a]IC_{50} for compounds **6d**, **6j** and miltefosine are represented as mean of three independent experiments.

The antileishmanial activity follows a trend for the corresponding pyrazolodihydropyridine and pyrazolopyridine compounds (Scheme 1).

In prototype I *i.e.* pyrazolodihydropyridines, by keeping a 1,3-diketone derived portion (dimedone) constant, the compounds (**6c, 6d** and **6e**) having electron-withdrawing groups (EWG) such as 4-chloro, 3,4-dichlorophenyl on R_1 and electron-donating groups (EDG) such as 2,5-dimethoxy, 3,4-dimethoxy, 3,4,5-trimethoxyphenyl on R_2 exhibited comparatively better (52-90%) inhibition at 25 and 50 μM concentrations against promastigotes with respect to other subprototypes. Compound **6d** displayed excellent antileishmanial activity against amastigotes (IC_{50} = 7.36 μM; CC_{50} = 497 μM; SI = 67) as compared to the standard drug miltefosine (IC_{50} = 9.46 μM; CC_{50} = 50 μM; SI = 5.3). Similar trends were observed in the case of compounds (**6g-6k**) derived from cyclopentane 1,3-dione, having EWG (4-fluoro, 4-chloro, 3,4-dichlorophenyl) on the R_1 and EDG (2,5-dimethoxy, 3,4-dimethoxy, 4-hydroxy-3,5-dimethoxyphenyl) on R_2 (Table 1 and 2). The compound **6j** having 3,4-dichlorophenyl on R_1 and 3,4-dimethoxy phenyl on R_2 showed excellent antileishmanial activity against amastigotes (IC_{50} = 4.05 μM; CC_{50} = 438

μM; SI = 108) as compared to the standard drug miltefosine (IC_{50} = 9.46 μM; CC_{50} = 50 μM; SI = 5.3).

In prototype II *i.e.* pyrazolopyridines, similar trends were observed as in the case of prototype I. Compounds (**7e-7k**) derived from dimedone possessing EWG (4-fluoro, 4-chloro, 3,4-dichlorophenyl) on R_1 and EDG (4-methoxy, 2,3-dimethoxy, 2,5-dimethoxy, 3,4-dimethoxy, 3,4,5-trimethoxyphenyl) on R_2 showed 41-90% inhibition against promastigotes. Compounds (**7l-7n**) having EWG (4-chloro, 3,4-dichlorophenyl) on the R_1 and EDG (2,5-dimethoxy, 3,4-dimethoxy, 3,4,5-trimethoxyphenyl) on R_2 showed 52-81% inhibition against promastigotes. Compounds (**7o-7s**) having EWG (4-fluoro, 4-chlorophenyl) on R_1 and EDG (4-methoxy, 2,5-dimethoxy, 3,4-dimethoxy, 2,3,4-trimethoxyphenyl) on R_2 showed 27-63% inhibition against promastigotes at 25 and 50 μM concentrations.

The effect of most active compounds (**6d** and **6j)** on the inhibition of promastigote and amastigote multiplication were also evaluated in a dose- and time-dependent manner by 3-(4,5-dimethylthiazol-2-yl)-2,5-diphenyltetrazolium bromide (MTT) assay and Giemsa staining, respectively. We observed >95% inhibition against promastigotes (Figure 2A) and >93% inhibition against intra-macrophagic amastigotes (Figure 2B) in 72 h. Next, the safety index (SI) of compounds **6d** and **6j** was investigated against both murine macrophages J774 and Vero cells. The different cell types were treated with increasing concentrations of **6d** and **6j** and the cytotoxicity was evaluated by MTT assay. Both compounds showed negligible toxicity against J774 and Vero cells up to 200 μM concentrations as >95% cells are viable (see the supporting information). The 50% inhibitory concentration (CC_{50}) of **6d** and **6j** was found to be >400 μM against both J774 and Vero cells (Table 2). The SI (CC_{50}/IC_{50}) of **6d** and **6j** was found to be 65.5 and 88.4 in J774 cells, respectively, and 67.6 and 108.2 in Vero cells, respectively (Table 2). So,

both these compounds were noncytotoxic and exhibited much higher safety index as compared to the standard drug miltefosine (SI = 5.8 and 5.3 in J774 and Vero cells, respectively; Table 2). Further to examine the effect of compounds on the growth pattern, promastigotes and intracellular amastigotes in macrophages were treated with various concentrations of **6d** and **6j**, ranging from 200 to 6.25 μM. It was observed that even at the lower concentrations (6.25 and 12.5 μM), these compounds arrested the parasitic growth (Figure 2C-F). The results motivated us to study the *in vitro* pharmacokinetics of compounds **6d** and **6j** prior to the *in vivo* studies in a murine model of visceral leishmaniasis.

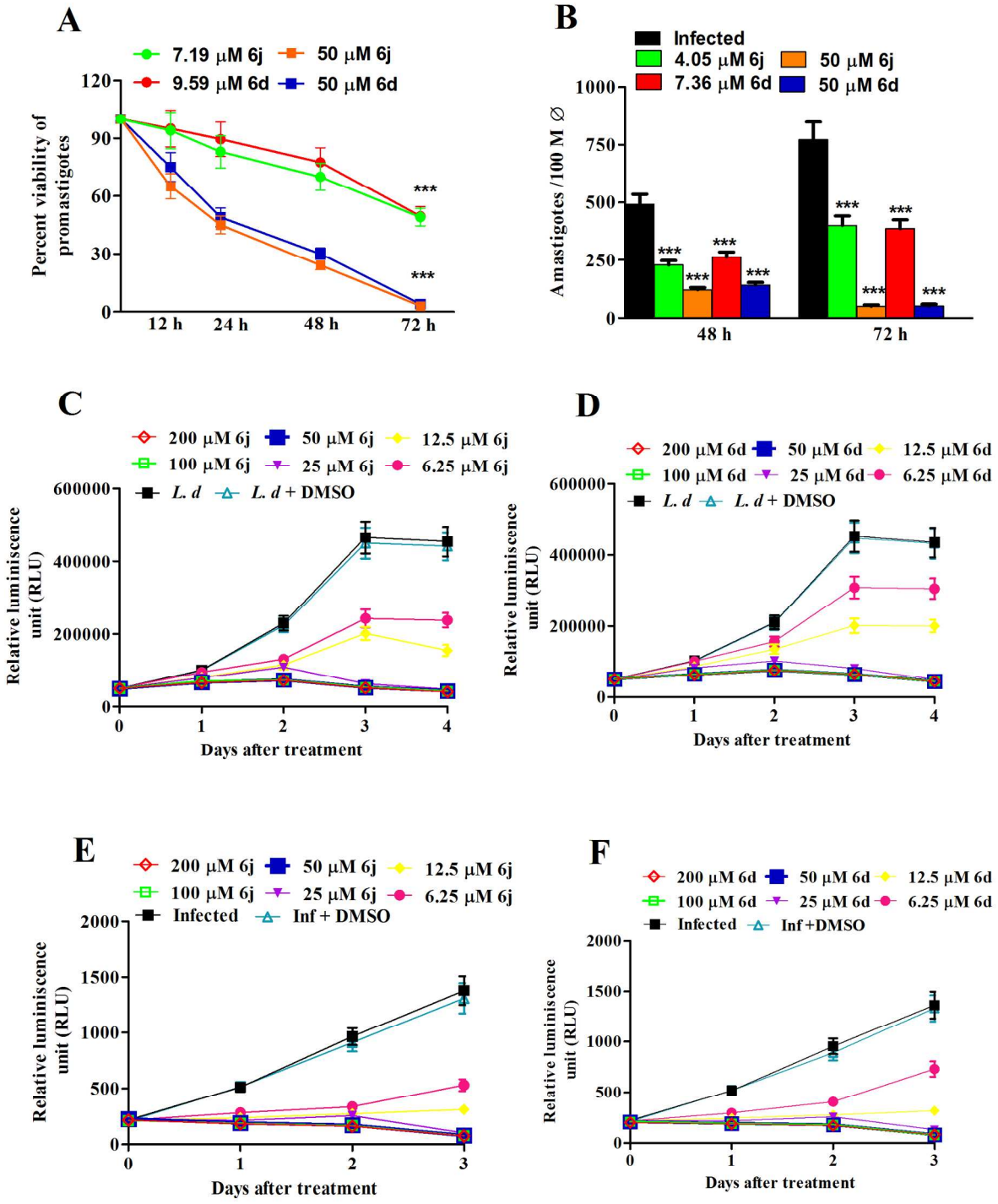

Figure 2. *In vitro* antileishmanial efficacy and cytotoxicity assessment of **6j** and **6d**. (A) Percent viability of promastigotes was evaluated by MTT method after treatment with IC_{50} and MIC of **6j** and **6d** for 12-72 h. (B) J774 macrophages were infected with promastigotes (1:8) as described in methods followed by treatment with IC_{50} and MIC doses of compounds **6j** and **6d**. The number of intra-macrophagic

amastigotes was determined by Giemsa staining. (C, D) Promastigotes were treated with various concentrations of **6j** (C) and **6d** (D) and cell viability was determined by luciferase activity. (E, F) Intracellular amastigotes were treated with same concentrations of **6j** (E) and **6d** (F) and parasitic growth was estimated on the basis of relative luminescence units in lysed macrophage cells. Data are representative of three independent experiments and results shown are means ± SD for each time point. Significance shown are for untreated vs treated groups, ***p<0.0001.

***In Vitro* Pharmacokinetic Study.** To assess the stability of the compounds in different conditions, **6d** and **6j** were studied in simulated gastric fluid (SGF, pH-1.2) and intestinal fluid (SIF, pH-6.5). The metabolic stability of the molecules was also assessed in mice S9 fraction to see the contribution of liver in the elimination of the compounds. Upon incubation with SGF, 85% of **6j**, and 75% of **6d** were found remaining intact after 120 min, suggesting that both these compounds would be stable in acidic pH that would be encountered in the stomach. Upon incubation with SIF, 99% of **6j** and 58% of **6d** were found remaining intact after 120 min, suggesting that compound **6d** is less stable in basic pH that would be encountered in the intestine. The representative plots of SGF and SIF stability are mentioned in Figure 3A and B. Around 45 and 31% of the parent compounds **6j** and **6d**, respectively, were found intact after 60 minutes of incubation with mice S9 fraction. *In vitro* metabolic half-life and rate constant for metabolism is given in Table 3 and the representative percent parent remaining vs time plots are given in Figure 3C. Based on the preclinical stability studies compound **6j** demonstrated better stability in different conditions compared to **6d**.

Table 3. *In Vitro* Metabolic Stability Parameters of 6j and 6d

parameter	**6j**	**6d**
k (min^{-1})	0.013	0.017

In vitro half-life, $t_{1/2}$ (min)	50.45	39.99
Intrinsic clearance, CL_{int} (μL/min/mg protein)	27.47	34.65

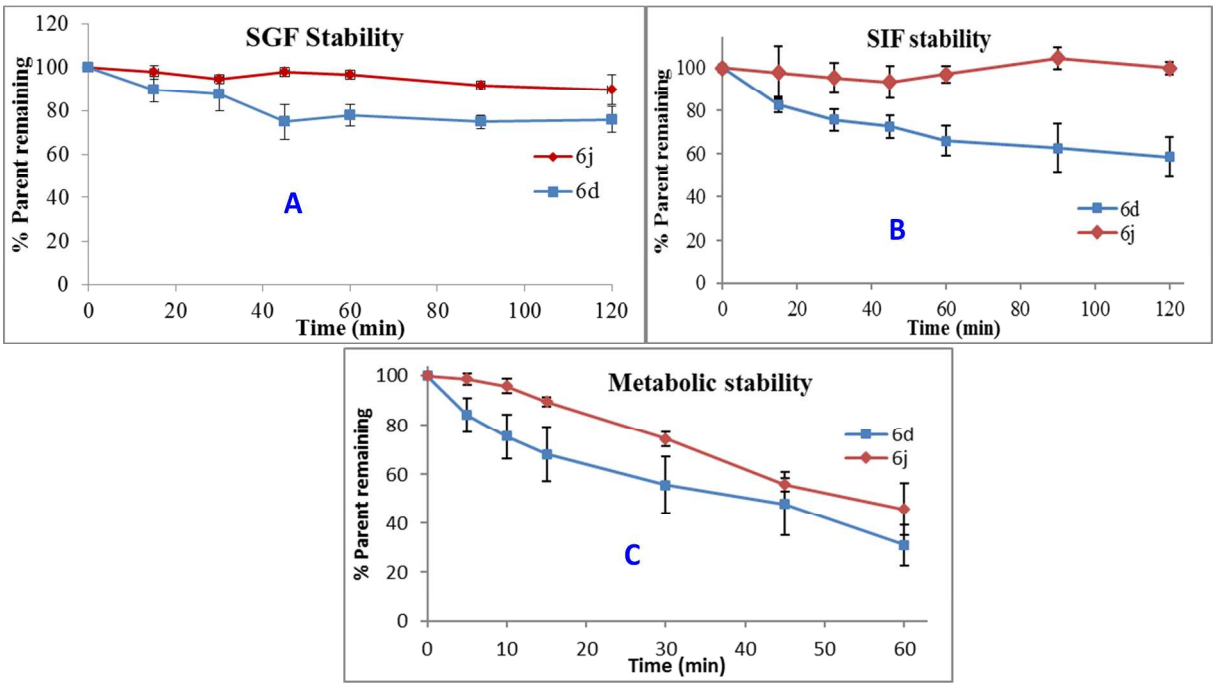

Figure 3. Percent parent remaining vs time plots of **6j** and **6d** upon incubation. (A) incubation in simulated gastric fluid. (B) incubation in simulated intestinal fluid. (C) incubation with mice S9 fraction.

***In Vivo* Activity and Combination Therapy of Compound 6j against *L. donovani*/Mice Model.** As described in materials and methods (experimental Section), compounds were administered intraperitoneally in mice infected with *L. donovani* with a dose range of 12.5-200 mg/kg/day for 5 consecutive days and sacrificed at day 7 after last treatment. The Parasitic burden was studied in liver and spleen smears. There was a clear dose oriented inhibition in the parasitic burden in the mice treated with **6d** and **6j** and both the compounds were seen to inhibit the parasitic burden in both liver and spleen (Figure 4A). But both compounds displayed different dose-response curves as **6j** showed better antileishmanial efficacy compared to **6d**. Compound **6j** showed >50% parasitic inhibition at a much lower dose of 25 mg/kg in both liver

and spleen whereas for **6d** at least 100 mg/kg was required to eliminate >50% parasite in both liver and spleen. Moreover, at a dose of 50 mg/kg/day for 5 days, **6j** showed >91 and >93% clearance in splenic and liver parasite burden, respectively (Figure 4A). Further increasing the dose of **6j** could not significantly enhance its therapeutic efficacy (90 and 92.7% in spleen and liver, respectively at 100 mg/kg and 90 and 93% in spleen and liver, respectively at 200 mg/kg) (Figure 4A). On the contrary, the maximum inhibition of liver and splenic parasite burden for **6d** was 62 and 68%, respectively at a much higher dose (200 mg/kg) (Figure 4A). As **6j** showed superior antileishmanial efficacy than **6d**, we performed time kinetics of organ parasite burden after **6j** treatment at its optimal dose *i.e.* 50 mg/kg. The compound was observed to inhibit the parasitic burden by >93% in both liver and spleen as early as 4 weeks post-infection *i.e.* almost one-week post-treatment (Figure 4B and C). However, increasing the time points did not significantly increase in the inhibition of parasitic burden in both liver and spleen as observed up to 7 weeks of post-treatment (Figure 4B and C).

Nowadays, in order to minimize the side effects caused by a drug, the combination therapy using a lower dose of standard drugs is going popular which reduces the dose, time and side effects. Despite its strong antileishmanial efficacy, standard oral drug miltefosine is demonstrated to have a serious side effect in human *i.e.* teratogenicity. It was observed that compounds **6d** and **6j** showed different dose-response curves whereas **6j** showed better antileishmanial efficacy compared to **6d**. We, therefore, thought it was worthwhile to check whether a lower dose of miltefosine in combination with **6j** could ameliorate *in vivo* parasite burden in BALB/c mice, similar to a higher curative dose of miltefosine. Percentage reduction in parasitic burden in the group treated with **6j (**25 mg/kg) was >59 and >48% in spleen and liver, respectively at day 7, so this dose was considered as a sub-curative (Figure 4D and E). A dramatic inhibition was

observed in parasitic burden in the infected groups treated with combination of sub-curative miltefosine (5 mg/kg) and **6j (**25 mg/kg) at both day 4 and day 7-post-treatment in liver and spleen (>92 and >97% inhibition, respectively as compared to infected mice) and the efficacy is well comparable with the curative dose of miltefosine *i.e.* 25 mg/kg (>98% inhibition in both liver and splenic parasite burden) (Figure 4D and E). Treatment with the sub-curative miltefosine resulted in a moderate parasitic inhibition in both liver (>75%) and spleen (>61%) at day 7 (Figure 4D and E). Throughout the course of the experiment at post-treatment, the animals seemed to be completely healthy with no variation in normal body weight. Both liver and spleen weights of the treated groups were significantly reduced compared to infected control after mono and combination therapy. All results showed better scope for combination therapy and motivated us to evaluate the status of host protective immune responses against VL in different experimental groups in detail.

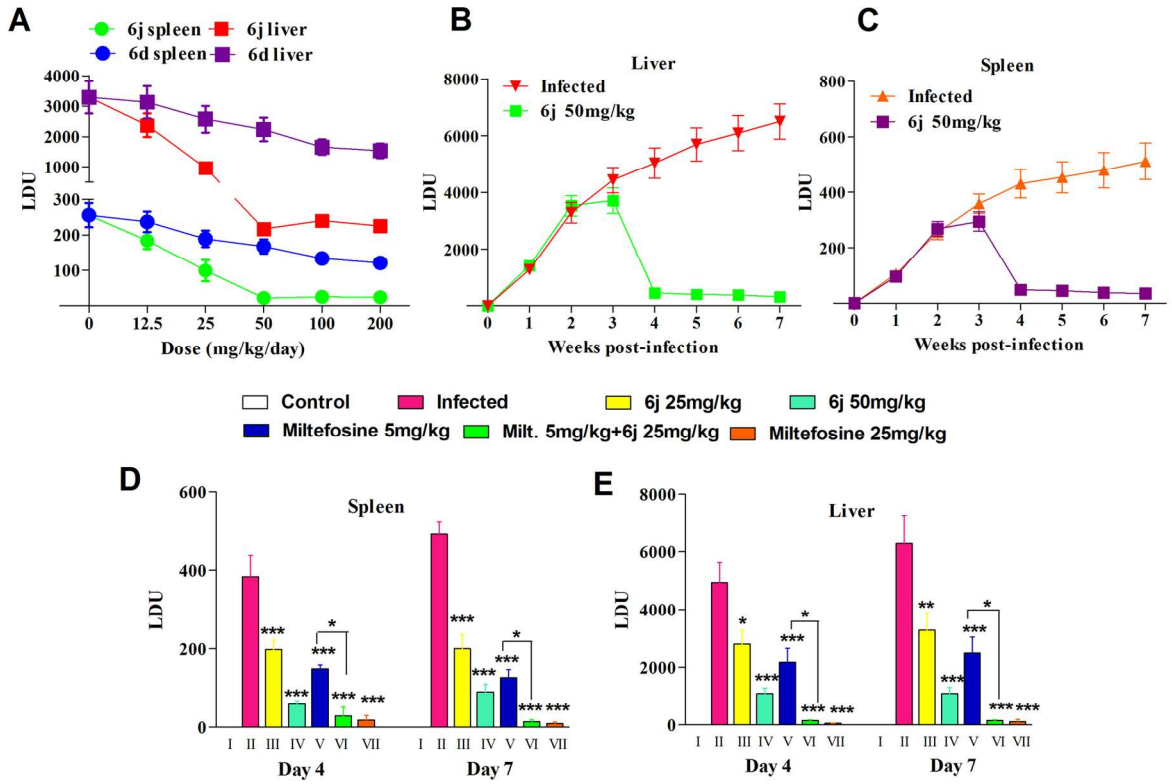

Figure 4. Effect of **6j** and **6d** monotherapy or combination therapy against on parasitic burden of *L. donovani* infected BALB/c mice. *L. donovani* infected mice were treated with various combinations of **6j**, **6d** and miltefosine as described in materials and method. (A) 15 days infected BALB/c mice were treated with different doses of **6j** and **6d** as indicated. Splenic and hepatic parasite loads were determined at day 7 post-treatment by a stamp-smear method**.** (4B-C) At various time points after treatments, mice of different experimental groups were sacrificed for determination of hepatic (B) and splenic (C) parasite loads by a stamp-smear method and expressed as Leishman Donovan units (LDU). (D-E) *L. donovani* infected mice were treated with various combinations of **6j** and miltefosine and splenic (D) and hepatic (E) parasitic burden was estimated as indicated. 1 LDU = amastigotes per nucleated cell × organ weight in milligrams. Data represents mean ± SD (n = 5 mice per group), representative of three independent experiments. Significance shown are for infected vs various treatment groups and sub-curative dose of miltefosine vs combination group, *$p < 0.05$, **$p < 0.005$, ***$p < 0.0001$.

Effect of Combination Therapy on T Cell Proliferation and Th1/Th2 Cytokine Balance *In Vivo*. Disease progression in VL is associated with impaired T cell proliferation and weak cell-mediated immunity, while disease healing demands higher T cell proliferation to exhibit the appropriate immune response. Therefore, the effect of combination therapy was investigated in the restoration of T cell proliferation in murine EVL. As observed, splenocytes isolated from *L. donovani* infected mice were unable to initiate T cell proliferation in the presence of SLA (soluble *L. donovani* promastigote antigen**)**. Whereas the groups treated with both sub-curative miltefosine (5 mg/kg) and **6j** (25 mg/kg) exhibited 9.9- and 8.4-fold increase in T cell proliferation compared to the infected group when stimulated by SLA at day 4 and day 7, respectively (Figure 5A). This was even higher than curative miltefosine (25 mg/kg) which resulted in 8.2- and 7.1-fold increase at day 4 and day 7, respectively. T cell proliferation was moderate (2.2- to 3.4-fold) in infected mice treated with lower doses of **6j** or sub-curative miltefosine cell proliferation (Figure 5A). *L. donovani* switches the Th1/Th2 cytokine balance towards anti-inflammatory Th2 mode to survive and propagate successfully inside its host.

Successful inhibition of the parasite demands higher levels of Th1 cytokines. A detailed splenic cytokine study was done to further assess the kind of immunological response in splenocytes of the mice with various treatment regimens. The cytokine profiling by ELISA revealed that the treatment with combination of sub-curative miltefosine and **6j** resulted in 9.1-, 7.4- and 12.7-fold increase in the level of IFN-γ, TNF-α and IL-12, respectively, at day 4 post-treatment which was 8.5-, 7.3- and 11.3-fold increase at day 7 post-treatment as compared to infected control (Figure 5B, C, and D). However, the same combination therapy resulted in 88 and 91% decreased at day 4 as well as 93- and 94%-fold decreased at day 7 in the level of TGF-β and IL-10, respectively (Figure 5E and F). These data were similar to cytokine secreted by infected mice treated with curative miltefosine (25 mg/kg) which resulted in 9.1-, 6.5- and 12.9-fold increase in the level of IFN-γ, TNF-α and IL-12 at day 4 while 8.1-, 5.3- and 9.5-fold increaseat day 7, respectively (Figure 5B, C and D). Similarly, curative miltefosine decreased the level of Th2 cytokine in infected mice likewise combination therapy group (87.5 and 88.7% decreases at day 4 as well as 94.6 and 92.9% decreases at day 7 in the level of TGF-β and IL-10, respectively) (Figure 5E and F). Sub-curative doses of miltefosine as well as **6j** showed a similar trend for Th1/Th2 cytokine synthesis but to lower extent which was consistent with their moderate inhibition of splenic and liver parasite burden. Collectively, these results suggest that in the *in vivo* situations, the combination of **6j** with sub-curative miltefosine restores T-cell proliferation towards host protective Th1 type thereby successfully eliminates the parasite from the infected mice.

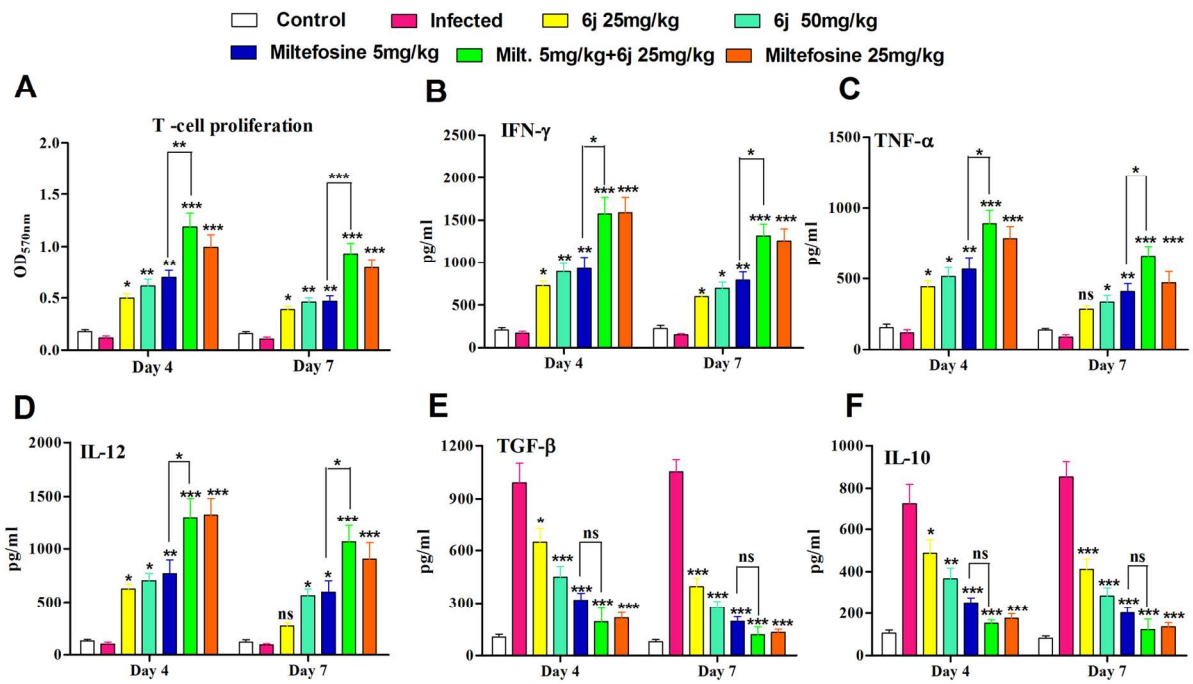

Figure 5. Effect of **6j**/miltefosine combination therapy on T-cell proliferation and Th1/Th2 cytokine balance in *L. donovani* infected BALB/c mice. Infected BALB/c mice were treated with different combinations of **6j** and miltefosine and splenocytes were isolated for assays. Isolated splenocytes from different groups on day 4 and day 7 post treatments were cultured and stimulated with 5 μg/ml soluble leishmanial antigen (SLA) for 72 h at 37 °C/5% CO_2 incubator. (A) T cell proliferation was assessed by MTT assay. (B-F) Supernatants from cultured splenocytes were evaluated for determination of IFN-γ (B), TNF-α (C), IL-12 (D), TGF-β (E) and IL-10 (F) levels by sandwich ELISA. Data represents mean ± SD (n = 5 mice per group), representative of three independent experiments. Significance shown are for infected vs various treatment groups and sub-curative dose of miltefosine vs combination group, *p < 0.05, **p < 0.005, ***p < 0.0001, *ns* = non-significant.

iNOS Expression and NO Generation Following Combination Therapy. iNOS mediated NO generation is crucial for controlling *Leishmania* infection in a murine model of EVL. Progression or healing of the disease depends on the nitrosative stress mediated by macrophage-derived NO critical for killing of intracellular *L. donovani* trapped in phagolysosomes. Therefore, the effect of combination therapy was explored on iNOS gene expression and NO generation. iNOS gene transcription in the murine splenocytes isolated from different treated groups coincided with the

level of pathogen clearance. The maximum increase in mRNA level was observed in the group treated with sub-curative doses of miltefosine plus **6j** (11.8- and 8.5- fold at day 4 and day 7, respectively) and curative miltefosine (12.3- and 9.1-fold at day 4 and day 7, respectively) (Figure 6A). This was fairly higher from the level of iNOS mRNA expression in infected animal treated with sub-curative miltefosine (6.4- and 3.4-fold at day 4 and day 7, respectively) and 25 mg/kg of **6j** (4.9- and 3.3-fold at day 4 and day 7, respectively) (Figure 6A). Similarly, NO generation in the culture supernatant of mice splenocytes from various therapeutic groups reflected the level of protection. *Leishmania* infection failed to induce nitrite production following SLA stimulation as expected while this was counteracted in the treated groups. The maximum generation of nitric oxide was seen in the mice treated with curative miltefosine as well as the mice treated with a combination of both sub-curative miltefosine and **6j (**25 mg/kg) at day 4 (7.4- and 5.6-fold increase, respectively compared to infected untreated) in SLA-stimulated splenocytes (Figure 6B). Similarly, the mice treated with 25 and 50 mg/kg of **6j** and sub-curative miltefosine showed significantly more nitric oxide compared to the infected control (4.1-, 4.7- and 4.3-fold increase, respectively (Figure 6B). These observations confirmed the heightened host immune-accessory functions of the infected animals undergoing combination therapy.

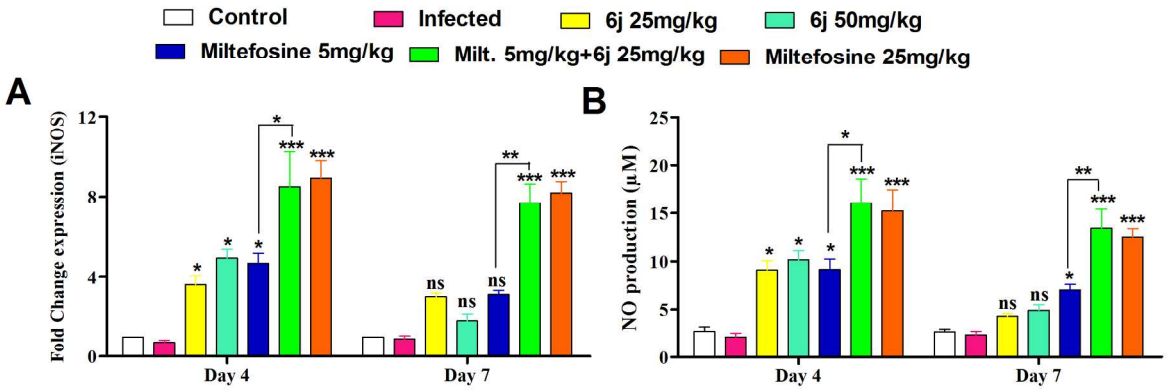

Figure 6. Effect of **6j**/miltefosine combination therapy on iNOS expression and NO generation in *L. donovani* infected BALB/c mice. (A) RNA was isolated from control, infected and treated BALB/c mice splenocytes on day 4 and day 7 post treatments and mRNA expression of iNOS was evaluated by real-time PCR. The mRNA level was normalized to mouse β-Actin and expressed as a fold change compared with uninfected controls. (B) Griess assay was performed to measure nitric oxide level in splenocytes supernatants from different groups of mice stimulated with SLA (5 μg/ml) for 72 h as described in methods. Data represents mean ± SD (n = 5 mice per group), representative of three independent experiments. Significance shown are for infected vs various treatment groups and sub-curative dose of miltefosine vs combination group, $*p < 0.05$, $**p < 0.005$, $***p < 0.0001$, *ns* = non-significant.

Induction of Apoptotic Cascades in *Leishmania donovani* Promastigotes Following Treatment with 6j. It is well established that cyclic pyrazole compounds induce apoptosis cascades in various cancer cells[20] and effective parasite suppression by compound **6j** in both *in vitro* and *in vivo* model of VL prompted us to investigate the programmed cell death mechanisms in *L. donovani* promastigotes. The flipping of phosphatidylserine from the inner leaflet to the outer leaflet of the plasma membrane is an early event of apoptosis. Using FITC conjugated annexin V which binds to phosphatidylserine and PI which binds to DNA in flow cytometry, three subpopulations can be distinguished, viable promastigotes (annexin V^-/PI^-), early apoptotic promastigotes (annexin V^+/PI^-) and late apoptotic or necrotic promastigotes (annexin V^+/PI^+). The Figure 7A clearly demonstrated that 38.2% of *L. donovani* promastigotes undergo apoptosis when treated for 48 h with IC_{50} dose of compound **6j** where 21% cells undergo late apoptosis and 17.2% cells are in early apoptotic phase. Furthermore, treatment with maximum inhibitory concentration (50 μM) of **6j** for 48 h induced 65.8% apoptosis in promastigotes where 11.6 and 54.2% cells are in early and late apoptotic cascade, respectively. On the contrary, only 8.2% of the parasite treated with vehicle (0.1% DMSO) undergoes apoptosis. DNA fragmentation is a hallmark feature of apoptosis in metazoan as well as unicellular protozoans, thus to further reconfirm apoptotic induction mediated by compound **6j** in the nuclear material of *L. donovani*

promastigotes, TUNEL assay was performed to detect the free ends of cleaved DNA fragments. As shown in Figure 7B, promastigotes incubated with both IC_{50} and 50 μM of compound **6j** showed a large number of bright fluorescent nuclei (indicating fragmentation of DNA) and significantly higher percentage of TUNEL positive cells as compared to the untreated and vehicle-treated promastigotes where fewer labeled nuclei were observed. In addition, bright field microscopic examination also showed that treated promastigotes were round in shape as compared to elongated and flagellated non-treated promastigotes.

Nevertheless, dysfunction of mitochondrial events has been shown to participate in the induction of apoptotic process. One of the early events responsible for induction of apoptosis cascade is a loss of MMP ($\Delta\Psi_m$) and it plays an important role in drug-induced death also in *Leishmania*.[21] To investigate whether compound **6j** treatment could disrupt MMP in *L. donovani* promastigotes, a time course study of $\Delta\Psi_m$ measurement was performed using the fluorescent dye, JC-1. JC-1 is a lipophilic cationic dye that fluoresces red upon aggregation in healthy cells, and however, after a loss of $\Delta\Psi_m$, it forms monomer throughout the cell and emits green fluorescence. We observed that incubation of promastigotes with compound **6j** at 50 μM for different time periods resulted in significant drop in transmembrane potential. Upon flow cytometric analysis it was observed that **6j** treatment to *L. donovani* promastigotes remarkably shift the fluorescence emission from red to green where 15.2% cells showed green fluorescence at 6 h post-treatment whereas 32.9 and 52.6% cells showed green fluorescence at 12 and 24 h, respectively (Figure 7C). On the contrary 5.02% of the parasite treated with vehicle (0.1% DMSO) showed green fluorescence at 24 h. Further incubation for 48 h lead to a little decrease in green fluorescence (44.9%) (Figure 7C). Taken together, we can conclude that compound **6j** induce disruption of $\Delta\Psi_m$ as an early event to trigger apoptosis of *Leishmania* parasite.

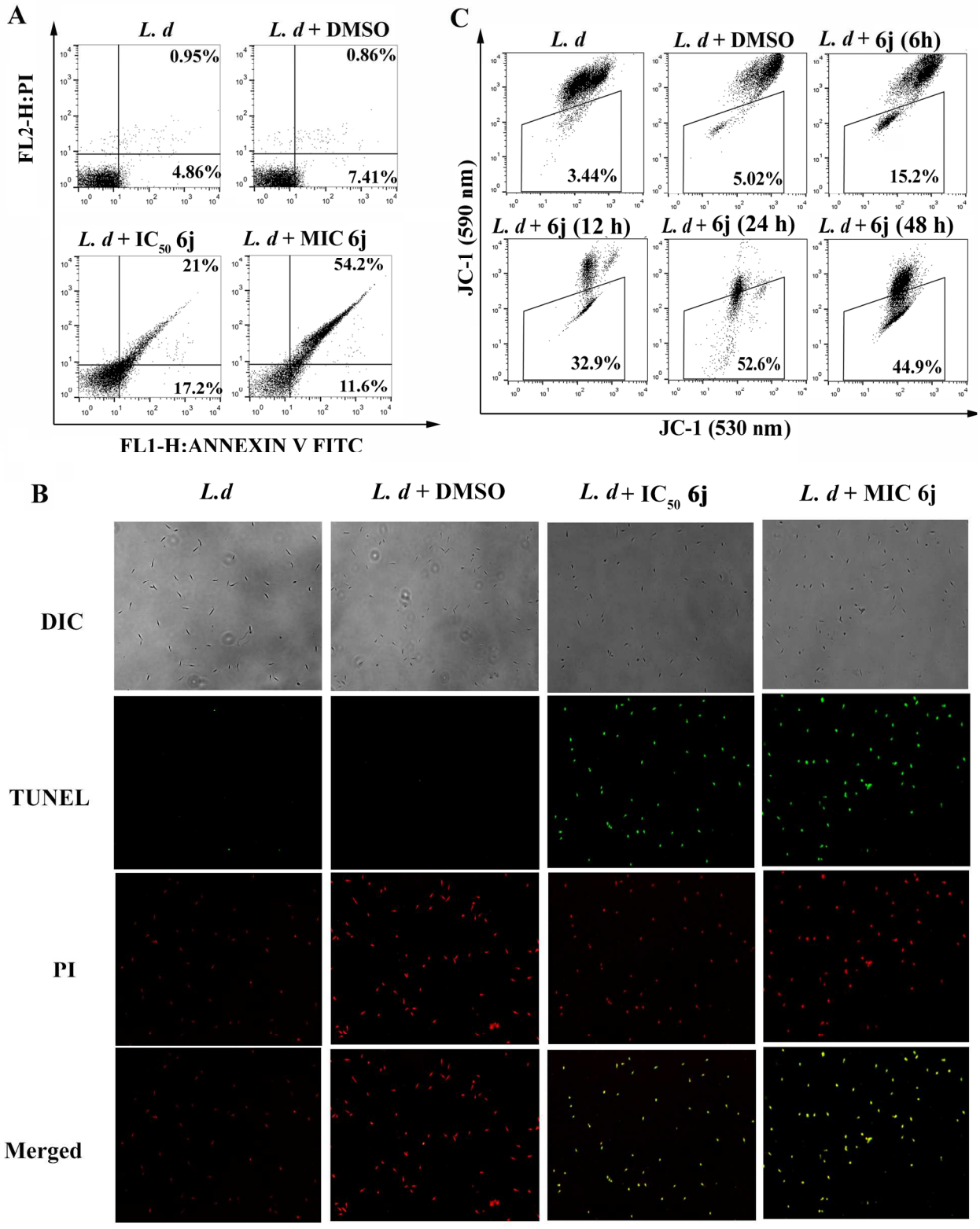
A
L. d
L. d + DMSO
0.95%
0.86%
4.86%
7.41%
L. d + IC50 6j
L. d + MIC 6j
21%
54.2%
17.2%
11.6%
FL2-H:PI
FL1-H:ANNEXIN V FITC
C
L. d
L. d + DMSO
L. d + 6j (6h)
3.44%
5.02%
15.2%
L. d + 6j (12 h)
L. d + 6j (24 h)
L. d + 6j (48 h)
32.9%
52.6%
44.9%
JC-1 (590 nm)
JC-1 (530 nm)
B
L.d
L. d + DMSO
L. d + IC50 6j
L. d + MIC 6j
DIC
TUNEL
PI
Merged

Figure 7. Compound **6j** induced apoptotic cell death cascade in *L. donovani* promastigotes. (A) Promastigotes were incubated with IC_{50} and MIC dose of compound **6j** (50 μM) and DMSO (0.1%) for 48 h co-stained with annexin V- FITC and propidium iodide. Stained promastigotes were analyzed using FACS Calibur Flow Cytometer and data was analyzed with Cell Quest software. (B) Exponential phase promastigotes were treated with compound **6j** (IC_{50} and MIC) for 48 h. Control promastigotes were treated with 0.1% DMSO containing M199 medium. Cells were observed under both phase contrast and fluorescent microscopy. Green color indicates TUNEL-positive *L. donovani* promastigotes (C) Exponential phase Dd8 promastigotes were treated with compound **6j** (50 μM) for 6-48 h and were labeled with potentiometric probe JC-1(2 μM final concentration).Time-dependent alterations in relative ($\Delta\Psi_m$) are expressed as the ratio of fluorescence measurements at 590 vs 530 nm. All results are representative of three independent experiments.

***In Vivo* Pharmacokinetic Study.** The mean plasma concentration-time profile of **6j** upon oral administration at a dose of 50 mg/kg is as shown in Figure 8 and its estimated pharmacokinetic parameters are represented in Table 4. Results show its faster absorption (T_{max}, 1.75 ± 0.50 h) with a peak plasma concentration level of 4.88 ± 0.61 μM (C_{max}). The time taken for the systemic levels to reduce to half (half-life, $t_{1/2}$) was 4.81 ± 0.29 h and the elimination rate constant (K_e) was found to be 0.14 ± 0.01 h^{-1}. The apparent volume of distribution was found to be 19.56 ± 2.36 L/kg and clearance was found to be 2.84 ± 0.48 L/h/kg indicating that the compound showed low clearance. The area under the concentration-time profile ($AUC_{0-\infty}$) representing the total systemic drug exposure was 31.67 ± 6.22 h*μM. The pharmacokinetic parameters indicate that the compound **6j** have better oral exposure and can be a better lead for further optimization.

Table 4. Pharmacokinetic Parameters of 6j upon Oral Administration at 50 mg/kg Dose. Data Represented as Mean ± S.D. (*n*=4)

Parameter	Estimate

K_e (1/h)	0.14 ± 0.01
$t_{1/2}$ (h)	4.81 ± 0.29
T_{max} (h)	1.75 ± 0.5
C_{max} (μM)	4.88 ± 0.61
AUC $_{0-\infty}$ (h*μM)	31.67 ± 6.22
V_d/F (L/kg)	19.56 ± 2.34
Cl/F (L/h/kg)	2.84 ± 0.48

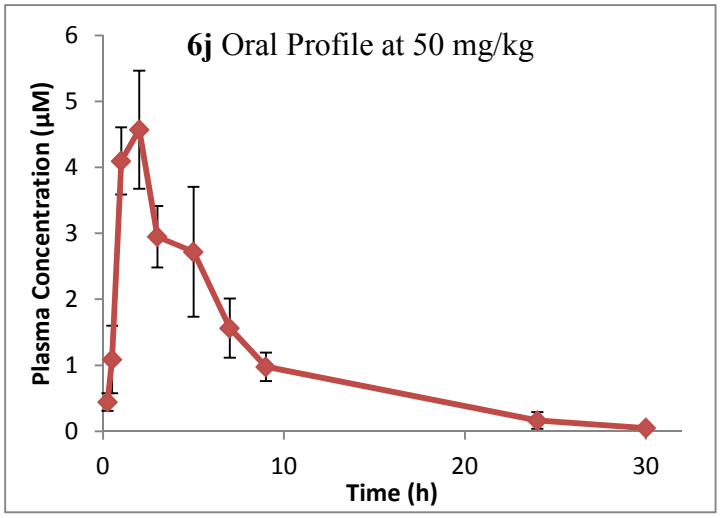

Figure 8. Mean plasma concentration- time profile of **6j** upon oral administration. Data represented as mean ± S.D. (*n*=4).

CONCLUSION

A series of pyrazolodihydropyridines and pyrazolopyridines were synthesized and tested for their *in vitro* antileishmanial activity against luciferase expressing *L. donovani.* Compounds **6d** and **6j** were found to be most promising as compared to the drug miltefosine. Compounds **6d** and **6j** exhibited much high SI value and good safety profile than miltefosine. The *in vivo* study of compounds **6d** and **6j** was performed in *L. donovani*/mice model via ip route, in which

compound **6j** showed better activity up to day 28 post-treatment as compared to the **6d**. The combination studies of the most active compound **6j** (25 mg/kg) and a sub-curative dose of miltefosine (5 mg/kg) exhibited comparable effects to that of a curative dose of standard marketed drug miltefosine (25 mg/kg) against *L. donovani* infected mice. The molecular and immunological studies showed that compound **6j** has a dual nature to act as a direct parasite killing agent as well as host immunostimulant. Pharmacokinetic parameters and *in vivo* studies of compound **6j** suggested that it may be a potential lead for further optimization to identify candidates for the treatment of the visceral leishmaniasis.

EXPERIMENTAL SECTION

General Methods. All reagents were purchased from commercial sources and used without further purification. Reactions were monitored by thin-layer chromatography (TLC) silica gel plates with fluorescence F_{254}. Melting points were taken in open capillaries on melting point apparatus and are presented uncorrected. Infrared spectra were recorded using FT-IR spectrophotometer. ^{1}H NMR spectra were recorded on a 300, 400 and 500 MHz Bruker Avance spectrometer and were determined in $CDCl_3$ and DMSO-d_6. ^{13}C NMR spectra were recorded in DMSO-d_6 and $CDCl_3$ on a 50, 75, 100, and 125 MHz Bruker Avance spectrometer. Two-dimensional (2D) experiment HSQC was performed on a 100 MHz Bruker Avance spectrometer. Chemical shifts are reported in parts per million. Splitting patterns are described as singlet (s), broad singlet (br s), doublet (d), broad doublet (br d), double doublet (dd), triplet (t), quartet (q), and multiplet (m). HRESIMS spectra were recorded using Q-TOF mass spectrometer. All tested compounds were ≥95% pure by HPLC with detection at 254 nm and 220 nm. The target compounds and substructures presented herein are not associated with commonly encountered

PAINS[22]. The potent compounds **6d** and **6j** passed the PAINS filter using SYBYL-X-2.1 (SYBYL-X Suite. available online: http://tripos.com).

General Procedure A. *Synthesis of 1-aryl-3-indolyl-5-amino pyrazoles (**3a-c**).* To a solution of 3-(cyanoacetyl)indole **2** (1.0 equiv.) in EtOH (20 mL) was added substituted phenylhydrazine hydrochloride (1.1 equiv) and *p*-TsOH.H_2O (0.3 equiv.). The reaction mixture was refluxed for 2 h. After completion of the reaction (monitored by TLC), the reaction mixture was cooled to room temperature and concentrated under reduced pressure. The residue was neutralized with a saturated $NaHCO_3$ solution (3 x 20 mL), extracted with EtOAc (3 x 20 mL), dried over anhydrous Na_2SO_4, and concentrated under reduced pressure. The pure 1-aryl-3-indolyl-5-amino pyrazole solid product (**3a-c)** was obtained after recrystallization in EtOH (20 mL).

General Procedure B. *Synthesis of Pyrazolodihydropyridine and Pyrazolopyridine derivatives.*

To a solution of 1-aryl-3-indolyl-5-amino pyrazole **3** (1.0 equiv.) in acetic acid (20 mL) was added cyclic 1,3-diketone **4** (1.0 equiv.) and aryl aldehyde **5** (1.0 equiv.). The reaction mixture was stirred at 100-110 °C for 2 h. After completion of the reaction (monitored by TLC), the reaction mixture was cooled to room temperature. It was diluted with water (15 mL) and neutralized with a saturated $NaHCO_3$ solution (3 x 20 mL), extracted with EtOAc (3 x 20 mL), dried over anhydrous sodium sulfate and concentrated under reduced pressure. The pure product Pyrazolodihydropyridine or pyrazolopyridine (**6** or **7**) was obtained after recrystallization in EtOH (20 mL).

General Procedure C. *DDQ oxidation of Pyrazolodihydropyridines.* To a solution of pyrazolodihydropyridine derivative **6** (1.0 equiv.) in CH_3CN (20 mL) was added DDQ (1.0 equiv.). Then, the reaction mixture was stirred at room temperature for 2-3 h. After completion of the reaction (monitored by TLC), the reaction mixture was diluted with water, extracted with

dichloromethane (3 x 20 mL), dried over anhydrous sodium sulfate and concentrated under reduced pressure. The crude product was purified by silica gel (60-120 mesh) column chromatography by using hexane: EtOAc (80: 20) as an eluent.

1-(4-Chlorophenyl)-3-(1H-indol-3-yl)-1H-pyrazol-5-amine (**3a**). The title compound was prepared according to General Procedure A using 3-(cyanoacetyl)indole **2** (300 mg, 1.63 mmol), 4-chlorophenyl hydrazine hydrochloride (321 mg, 1.79 mmol) and *p*-TsOH.H_2O (91 mg, 0.48 mmol) in EtOH to give **3a** (401 mg, 80%); white solid; mp > 270 °C; ^{1}H NMR (300 MHz, DMSO-d_6): δ = 11.22 (s, 1H), 8.18 (d, 1H, J = 7.2 Hz), 7.78 (d, 2H, J = 8.7 Hz), 7.71 (s, 1H), 7.56 (d, 2H, J = 9 Hz), 7.40 (d, 1H, J = 7.5 Hz), 7.15-7.04 (m, 2H), 5.86 (s, 1H), 5.45 (s, 2H) ppm; ^{13}C NMR (50 MHz, DMSO-d_6): δ = 148.0, 147.5, 138.6, 136.4, 129.4, 128.9, 124.9, 123.7, 123.5, 121.4, 121.2, 119.3, 111.5, 109.4, 87.9 ppm; FT-IR (KBr, ν_{max}/cm^{-1}) 3425, 1620, 1384, 1069, 669; HRMS (ESI): *m/z* calcd for $C_{17}H_{13}ClN_4$ $[M + H]^+$ 309.0907; found 309.0902.

1,4-Bis(4-chlorophenyl)-3-(1H-indol-3-yl)-7,7-dimethyl-6,7,8,9-tetrahydro-1H-pyrazolo[3,4-b]quinolin-5(4H)-one (**6a**). The title compound was prepared according to General Procedure B using 1-(4-chlorophenyl)-3-(1H-indol-3-yl)-1H-pyrazol-5-amine **3a** (300 mg, 0.97 mmol), dimedone (136 mg, 0.97 mmol) and 4-chloro benzaldehyde (136 mg, 0.97 mmol) in acetic acid to yield **6a** (430 mg, 80%); light yellow solid; mp >230 °C; ^{1}H NMR (400 MHz, DMSO-d_6): δ = 11.19 (s, 1H), 9.58 (s, 1H), 8.21 (d, 1H, J = 7.9 Hz), 7.75 (d, 2H, J = 8.8 Hz), 7.66 (d, 2H, J = 8.7 Hz), 7.43 (d, 1H, J = 2.6 Hz), 7.36-7.33 (m, 3H), 7.22 (d, 2H, J = 8.4 Hz), 7.12-7.08 (m, 1H), 7.03 (t, 1H, J = 7.8 Hz), 5.37 (s, 1H), 2.56-2.44 (m, 2H, overlapped with DMSO residual signal proved with HSQC), 2.20 (d, 1H, J = 16.1 Hz), 2.02 (d, 1H, J = 16.1 Hz), 1.0 (s, 3H), 0.82 (s, 3H) ppm; ^{13}C NMR (75 MHz, DMSO-d_6): δ = 193.9, 150.7, 145.4, 145.3, 137.5, 137.1, 135.8, 131.1, 130.1, 129.9, 129.3, 127.6, 125.1, 125.0, 124.3, 121.7, 119.4, 111.4, 109.9, 107.7,

101.5, 50.4, 48.5, 35.3, 31.9, 28.8, 26.3 ppm; FT-IR (KBr, ν_{max}/cm^{-1}) 3436, 2959, 1633, 771, 669; HRMS (ESI): *m/z* calcd for $C_{32}H_{26}Cl_2N_4O$ $[M + H]^+$ 553.1561; found: 553.1558.

4-(4-Chlorophenyl)-1-(4-fluorophenyl)-3-(1H-indol-3-yl)-7,7-dimethyl-6,7,8,9-tetrahydro-1H-pyrazolo[3,4-b]quinolin-5(4H)-one (**6b**). The title compound was prepared according to General Procedure B using 1-(4-fluorophenyl)-3-(1H-indol-3-yl)-1H-pyrazol-5-amine **3c** (300 mg, 1.02 mmol), dimedone (143 mg, 1.02 mmol) and 4-chloro benzaldehyde (143 mg, 1.02 mmol) in acetic acid to yield **6b** (427 mg, 78%); yellow solid; mp 230-232 °C; ^{1}H NMR (400 MHz, DMSO-d_6): δ = 11.17 (s, 1H), 9.56 (s, 1H), 8.21 (d, 1H, *J* = 7.9 Hz), 7.74 (dd, 2H, *J* = *8*.9, 4.9 Hz), 7.47-7.41 (m, 3H), 7.36-7.33 (m, 3H), 7.22 (d, 2H, *J* = 8.4 Hz), 7.10 (t, 1H, *J* = 7.6 Hz), 7.02 (t, 1H, *J* = 7.7 Hz), 5.37 (s, 1H), 2.56-2.44 (m, 2H, overlapped with DMSO residual signal proved with HSQC), 2.19 (d, 1H, *J* = 16.1 Hz), 2.02 (d, 1H, *J* = 16.0 Hz), 1.0 (s, 3H), 0.82 (s, 3H) ppm; ^{13}C NMR (75 MHz, DMSO-d_6): δ = 193.8, 160.8 ($J_{C\text{-}F}$ = 242.2 Hz), 150.8, 145.5, 144.9, 137.5, 135.8, 134.78, 134.75, 130.1, 129.9, 127.6, 125.8 ($J_{C\text{-}F}$ = 8.7 Hz), 125.1, 124.1, 121.7, 119.4, 116.2 ($J_{C\text{-}F}$ = 22.7 Hz), 111.3, 109.8, 107.8, 101.1, 50.4, 40.6, 35.3, 31.9, 28.8, 26.3 ppm; FT-IR (KBr, ν_{max}/cm^{-1}) 3429, 3019, 669, 622; HRMS (ESI): *m/z* calcd for $C_{32}H_{26}ClFN_4O$ $[M + H]^+$ 537.1857, found 537.1871.

1-(4-Chlorophenyl)-3-(1H-indol-3-yl)-7,7-dimethyl-4-(3,4,5-trimethoxyphenyl)-6,7,8,9-tetrahydro-1H-pyrazolo[3,4-b]quinolin-5(4H)-one (**6c**). The title compound was prepared according to General Procedure B using 1-(4-chlorophenyl)-3-(1H-indol-3-yl)-1H-pyrazol-5-amine **3a** (300 mg, 0.97 mmol), dimedone (136 mg, 0.97 mmol) and 3,4,5-trimethoxy benzaldehyde (191 mg, 0.97 mmol) in acetic acid to yield **6c** (474 mg, 80%); White solid; mp 274-276 °C; ^{1}H NMR (400 MHz, DMSO-d_6): δ = 11.28 (s, 1H), 9.53 (s, 1H), 8.13 (d, 1H, *J* = 7.8 Hz), 7.72 (d, 2H, *J* = 8.8 Hz), 7.66-7.64 (m, 3H), 7.39 (d, 1H, *J* = 8.0 Hz), 7.12 (t, 1H, *J* =

7.0 Hz), 7.04 (t, 1H, J = 7.8 Hz), 6.50 (s, 2H), 5.31 (s, 1H), 3.59 (s, 6H), 3.52 (s, 3H), 2.60-2.49 (m, 2H, overlapped with DMSO residual signal proved with HSQC), 2.23 (d, 1H, J = 16.1 Hz), 2.07 (d, 1H, J = 16.1 Hz), 1.03 (s, 3H), 0.95 (s, 3H) ppm; ^{13}C NMR (100 MHz, DMSO-d_6): δ = 194.0, 152.1, 151.0, 145.3, 142.6, 137.2, 137.1, 135.9, 135.4, 131.1, 129.3, 125.3, 124.9, 124.8, 121.6, 121.4, 119.4, 111.4, 110.0, 107.8, 105.1, 102.4, 59.8, 55.5, 50.4, 40.7, 35.8, 31.9, 29.1, 26.3 ppm; FT-IR (KBr, ν_{max}/cm^{-1}) 3435, 2085, 1635, 771, 673; HRMS (ESI): *m/z* calcd for $C_{35}H_{33}ClN_4O_4$ $[M + H]^+$ 609.2269, found 609.2270.

1-(3,4-Dichlorophenyl)-4-(2,5-dimethoxyphenyl)-3-(1H-indol-3-yl)-7,7-dimethyl-6,7,8,9-tetrahydro-1H-pyrazolo[3,4-b]quinolin-5(4H)-one (**6d**). The title compound was prepared according to General Procedure B using 1-(3,4-dichlorophenyl)-3-(1H-indol-3-yl)-1H-pyrazol-5-amine **3b** (300 mg, 0.87 mmol), dimedone (122 mg, 0.87 mmol) and 2,5-dimethoxy benzaldehyde (145 mg, 0.87 mmol) in acetic acid to yield **6d** (385 mg, 72%); yellow solid; HPLC: 95.6% pure; mp 203-205 °C; ^{1}H NMR (300 MHz, DMSO-d_6): δ = 11.31 (s, 1H), 9.48 (s, 1H), 8.20 (d, 1H, J = 7.5 Hz), 7.91 (s, 1H), 7.86-7.83 (m, 2H), 7.71 (d, 1H, J = 8.1 Hz), 7.35 (d, 1H, J = 7.8 Hz), 7.12-7.02 (m, 2H), 6.76 (d, 2H, J = 10.2 Hz), 6.57 (d, 1H, J = 8.4 Hz), 5.54 (s, 1H), 3.75 (s, 3H), 3.59 (s, 3H), 2.50 (s, 2H, overlapped with DMSO residual signal), 2.18 (d,1H, J = 15.9 Hz), 1.96 (d, 1H, J = 15.9 Hz), 1.02 (s, 3H), 0.88 (s, 3H) ppm; ^{13}C NMR (125 MHz, DMSO-d_6): δ = 193.7, 152.9, 151.2, 150.4, 146.0, 138.2, 137.9, 136.0, 131.8, 131.4, 129.0, 125.3, 125.2, 124.6, 123.3, 121.8, 121.7, 119.5, 116.8, 112.4, 111.4, 111.2, 107.7, 102.2, 56.2, 55.1, 50.6, 40.8, 32.0, 29.2, 26.1, 21.1 ppm; FT-IR (KBr, ν_{max}/cm^{-1}) 3435, 2918, 1219, 771, 673; HRMS (ESI): *m/z* calcd for $C_{34}H_{30}Cl_2N_4O_3$ $[M + H]^+$ 613.1773, found 613.1761.

1-(3,4-Dichlorophenyl)-4-(3,4-dimethoxyphenyl)-3-(1H-indol-3-yl)-7,7-dimethyl-6,7,8,9-tetrahydro-1H-pyrazolo[3,4-b]quinolin-5(4H)-one (**6e**). The title compound was prepared

according to General Procedure B using 1-(3,4-dichlorophenyl)-3-(1H-indol-3-yl)-1H-pyrazol-5-amine **3b** (300 mg, 0.87 mmol), dimedone (122 mg, 0.87 mmol) and 3,4-dimethoxy benzaldehyde (145 mg, 0.87 mmol) in acetic acid to yield **6e** (396 mg, 74%); white solid; mp >250 °C; ^{1}H NMR (400 MHz, DMSO-d_6): δ = 11.24 (s, 1H), 9.55 (s, 1H), 8.19 (d, 1H, J = 7.8 Hz), 7.95 (d, 1H, J = 2.3), 7.85 (d, 1H, J = 8.6 Hz), 7.73 (dd, 1H, J = 8.6, 2.2 Hz), 7.53 (d, 1H, J = 2.4 Hz), 7.37 (d, 1H, J = 7.9 Hz), 7.11 (t, 1H, J = 7.0 Hz), 7.05 (t, 1H, J = 7.6 Hz), 6.96 (s, 1H), 6.72 (s, 2H), 5.28 (s, 1H), 3.63 (s, 3H), 3.62 (s, 3H), 2.57-2.45 (m, 2H, overlapped with DMSO residual signal proved with HSQC), 2.20 (d, 1H, J = 16.1 Hz), 2.04 (d, 1H, J = 16.1 Hz), 1.02 (s, 3H), 0.88 (s, 3H) ppm; ^{13}C NMR (75 MHz, DMSO-d_6) δ = 194.0, 150.3, 147.8, 146.7, 145.8, 139.3, 138.1, 137.5, 135.9, 131.7, 131.2, 129.1, 125.1, 124.8, 123.4, 121.7, 121.5, 119.8, 119.5, 112.5, 111.4, 110.6, 107.6, 102.6, 55.38, 55.30, 50.4, 40.6, 35.1, 31.9, 28.9, 26.3 ppm; FT-IR (KBr, ν_{max}/cm^{-1}) 3443, 3335, 883, 831, 669, 586 cm-1; HRMS (ESI): *m/z* calcd for $C_{34}H_{30}Cl_2N_4O_3$ $[M + H]^+$ 613.1773, found 613.1796.

1-(4-Chlorophenyl)-3-(1H-indol-3-yl)-7,7-dimethyl-4-(thiophen-2-yl)-6,7,8,9-tetrahydro-1H-pyrazolo[3,4-b]quinolin-5(4H)-one (**6f**). The title compound was prepared according to General Procedure B using 1-(4-chlorophenyl)-3-(1H-indol-3-yl)-1H-pyrazol-5-amine **3a** (300 mg, 0.97 mmol), dimedone (136 mg, 0.97 mmol) and thiophene-2-carbaldehyde (109 mg, 0.97 mmol) in acetic acid to yield **6f** (281 mg, 55%); yellow solid; mp 208-210 °C; ^{1}H NMR (300 MHz, DMSO-d_6): δ = 11.22 (s, 1H), 9.64 (s, 1H), 8.26 (d, 1H, J = 7.5 Hz), 7.73 (d, 2H, J = 8.7 Hz), 7.65 (d, 2H, J = 8.7 Hz), 7.40-7.37 (m, 2H), 7.17-7.03 (m, 3H), 6.80 (br s, 2H), 5.65 (s, 1H), 2.50 (s, 2H, overlapped with DMSO residual signal), 2.25 (d, 1H, J = 16.2 Hz), 2.12 (d, 1H, J = 16.2 Hz), 1.01 (s, 3H), 0.89 (s, 3H) ppm; ^{13}C NMR (125 MHz, DMSO-d_6): δ = 194.1, 151.0, 145.5, 137.3, 137.2, 136.0, 131.2, 129.5, 126.3, 125.2, 125.0, 124.3, 124.0, 123.8, 121.9, 121.7,

119.6, 111.5, 109.9, 107.8, 101.6, 50.3, 40.6, 32.0, 30.8, 28.9, 26.5 ppm; FT-IR (KBr, ν_{max}/cm^{-1}) 3449, 2957, 964, 672; HRMS (ESI): *m/z* calcd for $C_{30}H_{25}ClN_4OS$ $[M + H]^+$ 525.1516, found 525.1542.

1-(4-Chlorophenyl)-4-(2,5-dimethoxyphenyl)-3-(1H-indol-3-yl)-4,6,7,8-tetrahydrocyclopenta[e]pyrazolo[3,4-b]pyridin-5(1H)-one (**6g**). The title compound was prepared according to General Procedure B using 1-(4-chlorophenyl)-3-(1H-indol-3-yl)-1H-pyrazol-5-amine **3a** (300 mg, 0.97 mmol), cyclopentane-1,3-dione (95 mg, 0.97 mmol) and 2,5-dimethoxy benzaldehyde (161mg, 0.97 mmol) in acetic acid to yield **6g** (366 mg, 70%); yellow solid; mp 174-176 °C; ^{1}H NMR (300 MHz, DMSO-d_6): δ = 11.26 (s, 1H), 10.16 (s, 1H), 8.24 (d, 1H, J = 6.9 Hz), 7.75-7.68 (m, 4H), 7.58 (br s, 1H), 7.32 (d, 1H, J = 6.9 Hz), 7.08-7.01 (m, 2H), 6.85 (d, 1H, J = 7.2 Hz), 6.62 (br s, 2H), 5.42 (s, 1H), 3.85 (s, 3H), 3.56 (s, 3H), 2.66 (s, 2H), 2.26 (s, 2H) ppm; ^{13}C NMR (100 MHz, DMSO-d_6): δ = 200.0, 165.9, 153.2, 150.5, 145.9, 138.9, 137.1, 135.9, 135.6, 131.2, 129.5, 125.2, 124.9, 124.6, 121.9, 121.6, 119.4, 116.8, 116.4, 112.8, 111.2, 110.8, 107.9, 101.8, 56.7, 55.0, 33.9, 29.2, 24.2 ppm; FT-IR (KBr, ν_{max}/cm^{-1}) 3437, 2142, 1528, 671; HRMS (ESI): *m/z* calcd for $C_{31}H_{25}ClN_4O_3$ $[M + H]^+$ 537.1693; found: 537.1686.

1-(4-Chlorophenyl)-3-(1H-indol-3-yl)-4-(3,4,5-trimethoxyphenyl)-4,6,7,8-tetrahydrocyclopenta[e]pyrazolo[3,4-b]pyridin-5(1H)-one (**6h**). The title compound was prepared according to General Procedure B using 1-(4-chlorophenyl)-3-(1H-indol-3-yl)-1H-pyrazol-5-amine **3a** (300 mg, 0.97 mmol), cyclopentane-1,3-dione (95 mg, 0.97 mmol) and 3,4,5-trimethoxy benzaldehyde (191 mg, 0.97 mmol) in acetic acid to yield **6h** (436 mg, 79%); yellow solid; mp 223-225 °C; ^{1}H NMR (300 MHz, DMSO-d_6): δ = 11.23 (s, 1H), 10.28 (s, 1H), 8.25 (d, 1H, J = 7.5 Hz), 7.76 (d, 2H, J = 8.7 Hz), 7.68 (d, 2H, J = 8.7 Hz), 7.36-7.34 (m, 2H), 7.14-7.03 (m, 2H), 6.62 (s, 2H), 5.18 (s, 1H), 3.62 (s, 6H), 3.57 (s, 3H), 2.66 (s, 2H), 2.35 (s, 2H)

ppm; ^{13}C NMR (75 MHz, DMSO-d_6): δ = 200.5, 165.9, 152.4, 146.1, 140.8, 138.8, 137.0, 135.8, 131.3, 129.4, 125.2, 125.0, 124.8, 121.6, 119.4, 115.6, 111.3, 107.7, 105.4, 101.0, 59.8, 55.7, 35.7, 33.9, 24.1 ppm; FT-IR (KBr, ν_{max}/cm^{-1}) 3299, 3229, 3021, 1216, 670, 506; HRMS (ESI): *m/z* calcd for $C_{32}H_{27}ClN_4O_4$ $[M + H]^+$ 567.1799; found: 567.1811.

1-(4-Chlorophenyl)-4-(4-hydroxy-3,5-dimethoxyphenyl)-3-(1H-indol-3-yl)-4,6,7,8-tetrahydrocyclopenta[e]pyrazolo[3,4-b]pyridin-5(1H)-one (**6i**). The title compound was prepared according to General Procedure B using 1-(4-chlorophenyl)-3-(1H-indol-3-yl)-1H-pyrazol-5-amine **3a** (300 mg, 0.97 mmol), cyclopentane-1,3-dione (95 mg, 0.97 mmol) and 4-hydroxy-3,5-dimethoxy benzaldehyde (177 mg, 0.97 mmol) in acetic acid to yield **6i** (364 mg, 66%); yellow solid; mp 270-272 °C; ^{1}H NMR (300 MHz, DMSO-d_6): δ = 11.18 (s, 1H), 10.21 (s, 1H), 8.24 (d, 1H, J = 7.5 Hz), 8.05 (s, 1H), 7.77-7.66 (m, 4H), 7.34 (d, 1H, J = 7.7 Hz), 7.27 (s, 1H), 7.13- 7.02 (m, 2H), 6.57 (s, 2H), 5.10 (s, 1H), 3.61 (s, 6H), 2.65 (br s, 2H), 2.33 (br s, 2H) ppm; ^{13}C NMR (75 MHz, DMSO-d_6): δ = 200.5, 165.5, 147.5, 146.2, 138.8, 137.0, 135.8, 135.4, 134.0, 131.2, 129.4, 125.2, 124.9, 124.8, 121.6, 119.4, 116.0, 111.3, 107.7, 105.9, 101.3, 55.9, 35.4, 33.9, 24.1 ppm; FT-IR (KBr, ν_{max}/cm^{-1}) 3305, 3019, 2400, 929, 757, 669; HRMS (ESI): *m/z* calcd for $C_{31}H_{25}ClN_4O_4$ $[M + H]^+$ 553.1643; found: 553.1645.

1-(3,4-Dichlorophenyl)-4-(3,4-dimethoxyphenyl)-3-(1H-indol-3-yl)-4,6,7,8-tetrahydrocyclopenta[e]pyrazolo[3,4-b]pyridin-5(1H)-one (**6j**). The title compound was prepared according to General Procedure B using 1-(3,4-dichlorophenyl)-3-(1H-indol-3-yl)-1H-pyrazol-5-amine **3b** (300 mg, 0.87 mmol), cyclopentane-1,3-dione (85 mg, 0.87 mmol) and 3,4-dimethoxy benzaldehyde (145mg, 0.87 mmol) in acetic acid to yield **6j** (354 mg, 71%); light yellow solid; HPLC: 98% pure; mp >270 °C; ^{1}H NMR (300 MHz, DMSO-d_6): δ = 11.18 (s, 1H), 10.30 (s, 1H), 8.24 (d, 1H, J = 7.5 Hz), 7.98 (d, 1H, J = 2.4 Hz), 7.88 (d, 1H, J = 8.7 Hz), 7.77-

7.74 (m, 1H), 7.34-7.28 (m, 2H), 7.10-7.03 (m, 3H), 6.75-6.67 (m, 2H), 5.13 (s, 1H), 3.67 (s, 3H), 3.63 (s, 3H), 2.65 (s, 2H), 2.32 (s, 2H) ppm; ^{13}C NMR (75 MHz, DMSO-d_6): δ = 200.5, 165.4, 148.0, 147.0, 146.6, 139.1, 137.9, 137.8, 135.8, 131.8, 131.3, 129.3, 125.2, 125.0, 124.9, 123.5, 121.7, 119.8, 119.5, 116.2, 112.7, 111.6, 111.3, 107.5, 101.5, 55.4, 55.3, 35.2, 33.9, 24.1 ppm; FT-IR (KBr, ν_{max}/cm^{-1}) 3435, 3019, 770, 669, 625; HRMS (ESI): *m/z* calcd for $C_{31}H_{24}Cl_2N_4O_3$ $[M + H]^+$ 571.1304; found: 571.1322.

1-(4-Fluorophenyl)-4-(4-hydroxy-3,5-dimethoxyphenyl)-3-(1H-indol-3-yl)-4,6,7,8-tetrahydrocyclopenta[e]pyrazolo[3,4-b]pyridin-5(1H)-one (**6k**). The title compound was prepared according to General Procedure B using 1-(4-fluorophenyl)-3-(1H-indol-3-yl)-1H-pyrazol-5-amine **3c** (300 mg, 1.02 mmol), cyclopentane-1,3-dione (100 mg, 1.02 mmol) and 4-hydroxy-3,5-dimethoxy benzaldehyde (186 mg, 1.02 mmol) in acetic acid to yield **6k** (350 mg, 64%); yellow solid; mp >270 °C; ^{1}H NMR (300 MHz, DMSO-d_6): δ = 11.17 (s, 1H), 10.19 (s, 1H), 8.23 (d, 1H, J = 7.5 Hz), 8.07 (s, 1H), 7.78-7.73 (m, 2H), 7.49-7.44 (m, 2H), 7.33 (d, 1H, J = 7.8 Hz), 7.26 (d, 1H, J = 2.1 Hz), 7.12-7.01 (m, 2H), 6.56 (s, 2H), 5.09 (s, 1H), 3.60 (s, 6H), 2.64 (s, 2H), 2.32 (s, 2H) ppm; ^{13}C NMR (75 MHz, DMSO-d_6): δ = 200.5, 165.6, 160.8 ($J_{C\text{-}F}$ = 242.8 Hz), 147.6, 145.9, 138.8, 135.8, 135.6, 134.7, 134.0, 125.7 ($J_{C\text{-}F}$ = 8.7 Hz), 125.3, 124.7, 121.6 ($J_{C\text{-}F}$ = 4.1 Hz), 119.4, 116.3 ($J_{C\text{-}F}$ = 22.9 Hz), 116.0, 111.3, 107.9, 105.9, 101.0, 56.0, 35.4, 33.9, 30.6 ppm; FT-IR (KBr, ν_{max}/cm^{-1}) 3290, 3021, 1103, 764, 669; HRMS (ESI): *m/z* calcd for $C_{31}H_{25}FN_4O_4$ $[M + H]^+$ 537.1938; found 537.1937.

1,4-Bis(4-chlorophenyl)-3-(1H-indol-3-yl)-4,10-dihydroindeno[2,1-e]pyrazolo[3,4-b]pyridin-5(1H)-one (**6l**). The title compound was prepared according to General Procedure B using 1-(4-chlorophenyl)-3-(1H-indol-3-yl)-1H-pyrazol-5-amine **3a** (300 mg, 0.97 mmol), 1,3-indanedione (142 mg, 0.97 mmol) and 4-chloro benzaldehyde (136 mg, 0.97 mmol) in acetic acid to yield **6l**

(375 mg, 69%); red solid; mp 174-176 °C; ^{1}H NMR (500 MHz, DMSO-d_6): δ = 11.20 (s, 1H), 10.84 (s, 1H), 8.23 (d, 1H, J = 7.8 Hz), 7.85 (d, 2H, J = 7.5 Hz), 7.71 (d, 3H, J = 8.3 Hz), 7.42-7.36 (m, 4H), 7.33-7.31 (m, 2H), 7.25-7.24 (m, 3H), 7.11-7.01 (m, 2H), 5.41 (s, 1H) ppm; 13C NMR (75 MHz, DMSO-d_6): δ = 190.3, 155.0, 146.2, 143.9, 138.5, 137.2, 136.4, 135.8, 133.9, 131.8, 131.4, 130.7, 130.0, 129.5, 127.9, 125.8, 125.1, 124.9, 121.7, 120.1, 119.5, 111.3, 108.4, 107.3, 102.2, 34.8 ppm; FT-IR (KBr, v_{max}/cm^{-1}) 3438, 2920, 1150, 770; HRMS (ESI): *m/z* calcd for $C_{33}H_{20}Cl_2N_4O$ $[M + H]^+$ 559.1092 found: 559.1099.

4-(4-Chlorophenyl)-1-(4-fluorophenyl)-3-(1H-indol-3-yl)-4,10-dihydroindeno[2,1-e]pyrazolo[3,4-b]pyridin-5(1H)-one (**6m**). The title compound was prepared according to General Procedure B using 1-(4-fluorophenyl)-3-(1H-indol-3-yl)-1H-pyrazol-5-amine **3c** (300 mg, 1.02 mmol), 1,3-indanedione (150 mg, 1.02 mmol) and 4-chloro benzaldehyde (143 mg, 1.02 mmol) in acetic acid to yield **6m** (380 mg, 72%); red solid; mp >270 °C; ^{1}H NMR (300 MHz, DMSO-d_6): δ = 11.18 (s, 1H), 10.82 (s, 1H), 8.23 (d, 1H, J = 6.9 Hz), 7.86 (br s, 2H), 7.73 (d, 1H, J = 6.3 Hz), 7.53-7.24 (m, 11 H), 7.09-7.02 (m, 2H), 5.42 (s, 1H) ppm. ^{13}C NMR (75 MHz, DMSO-d_6): δ = 190.2, 161.1 ($J_{C\text{-}F}$ = 243.2 Hz), 155.0, 145.8, 144.0, 138.5, 136.3, 135.7, 134.8, 133.9, 131.3, 130.6, 130.0, 127.9, 126.5 ($J_{C\text{-}F}$ = 7.5 Hz), 125.1, 124.7, 121.7 ($J_{C\text{-}F}$ = 4.5 Hz), 120.1, 119.4, 116.2 ($J_{C\text{-}F}$ = 22.7 Hz), 111.3, 108.3, 107.4, 101.8, 34.8 ppm; FT-IR (KBr, v_{max}/cm^{-1}) 3435, 2143, 1639, 668, 515; HRMS (ESI): *m/z* calcd for $C_{33}H_{20}ClFN_4O$ $[M + H]^+$ 543.1388; found: 543.1385.

1-(4-Chlorophenyl)-3-(1H-indol-3-yl)-4-(2,3,4-trimethoxyphenyl)-4,10-dihydroindeno[2,1-e]pyrazolo[3,4-b]pyridin-5(1H)-one (**6n**). The title compound was prepared according to General Procedure B using 1-(4-chlorophenyl)-3-(1H-indol-3-yl)-1H-pyrazol-5-amine **3a** (300 mg, 0.97 mmol), 1,3-indanedione (142 mg, 0.97 mmol) and 2,3,4-trimethoxy benzaldehyde (190

mg, 0.97 mmol) in acetic acid to yield **6n** (419 mg, 70%); yellow solid; mp 260-262 °C; ^{1}H NMR (300 MHz, DMSO-d_6): δ = 11.33 (s, 1H), 10.73 (s, 1H), 8.26 (d, 1H, J = 7.8 Hz), 7.83 (d, 2H, J = 8.1 Hz), 7.73-7.71 (m, 4H), 7.43-7.29 (m, 3H), 7.22 (d, 1H, J = 6.6 Hz), 7.10-6.98 (m, 2H), 6.88 (d, 1H, J = 8.4 Hz), 6.58 (d, 1H, J = 8.7 Hz), 5.51 (s, 1H), 4.09 (s, 3H), 3.71 (s, 3H), 3.63 (s, 3H) ppm. ^{13}C NMR (75 MHz, DMSO-d_6): δ = 190.3, 155.1, 151.5, 150.1, 146.0, 140.9, 138.2, 137.2, 136.6, 135.8, 135.6, 133.9, 131.5, 131.3, 131.2, 129.8, 129.4, 129.3, 125.5, 125.2, 124.8, 124.3, 122.6, 121.8, 121.5, 119.9, 119.3, 111.1, 109.4, 107.8, 107.5, 103.4, 60.6, 60.0, 55.5 ppm; FT-IR (KBr, ν_{max}/cm^{-1}) 3684, 3619, 770, 669, 625; HRMS (ESI): *m/z* calcd for $C_{36}H_{27}ClN_4O_4$ $[M + H]^+$ 615.1799; found: 615.1803.

1-(4-Chlorophenyl)-3-(1H-indol-3-yl)-4-(thiophen-2-yl)-4,10-dihydroindeno[2,1-e]pyrazolo[3,4-b]pyridin-5(1H)-one (**6o**). The title compound was prepared according to General Procedure B using 1-(4-chlorophenyl)-3-(1H-indol-3-yl)-1H-pyrazol-5-amine **3a** (300 mg, 0.97 mmol), 1,3-indanedione (142 mg, 0.97 mmol) and thiophene-2-carbaldehyde (109 mg, 0.97 mmol) in acetic acid to yield **6o** (298 mg, 58%); red solid; mp 154-155 °C; ^{1}H NMR (300 MHz, DMSO-d_6): δ = 11.26 (s, 1H) 10.88 (s, 1H), 8.27 (d, 1H, J = 7.2 Hz), 7.82 (d, 2H, J = 7.8 Hz), 7.73-7.70 (m, 3H), 7.48-7.31 (m, 5H), 7.19-7.03 (m, 4H), 6.84 (m, 1H), 5.68 (s, 1H) ppm; ^{13}C NMR (75 MHz, DMSO-d_6) δ = 190.1, 154.9, 150.0, 146.3, 137.9, 137.1, 136.3, 135.8, 133.9, 131.7, 131.5, 130.0, 129.5, 126.5, 125.7, 125.2, 124.9, 124.4, 124.2, 121.7, 120.2, 119.5, 111.3, 108.3, 107.4, 102.7, 30.2 ppm; FT-IR (KBr, ν_{max}/cm^{-1}) 3438, 1633, 1195, 1149, 1097, 690; HRMS (ESI): *m/z* calcd for $C_{31}H_{19}ClN_4OS$ $[M + H]^+$ 531.1046, found 531.1042.

1-(4-Chlorophenyl)-4-(2,4-dichlorophenyl)-3-(1H-indol-3-yl)-7,7-dimethyl-7,8-dihydro-1H-pyrazolo[3,4-b]quinolin-5(6H)-one (**7a**). The title compound was prepared according to General Procedure B using 1-(4-chlorophenyl)-3-(1H-indol-3-yl)-1H-pyrazol-5-amine **3a** (300 mg, 0.97

mmol), dimedone (136 mg, 0.97 mmol) and 2,4-dichloro benzaldehyde (170 mg, 0.97 mmol) in acetic acid to yield **7a** (405 mg, 71%); yellow solid; mp 240-242 °C; ^{1}H NMR (400 MHz, $CDCl_3$): δ = 8.49-8.46 (m, 2H), 8.05 (s, 1H), 7.80 (d, 1H, J = 7.9 Hz), 7.54-7.50 (m, 2H), 7.31 (d, 1H, J = 8.1 Hz), 7.24-7.19 (m, 2H), 7.14-7.10 (m, 1H), 6.87-6.82 (m, 2H), 6.38 (d, 1H, J = 2.6 Hz), 3.29 (s, 2H), 2.62 (d, 1H, J = 16.2 Hz), 2.50 (d, 1H, J = 16.3 Hz), 1.18 (s, 3H), 1.17 (s, 3H) ppm; ^{13}C NMR (75 MHz, DMSO-d_6) δ = 196.5, 163.5, 150.0, 143.4, 143.1, 137.5, 135.3, 134.8, 133.0, 132.1, 130.8, 130.2, 129.2, 128.0, 126.5, 126.2, 125.6, 122.2, 121.7, 120.3, 120.1, 119.5, 114.4, 111.3, 105.8, 55.9, 52.8, 47.5, 31.8, 27.8, 27.2 ppm; FT-IR (KBr, ν_{max}/cm-1) 3396, 2921, 1097, 768; HRMS (ESI): *m/z* calcd for $C_{32}H_{23}Cl_3N_4O$ $[M + H]^+$ 585.1016, found 585.1000.

4-(2,4-Dichlorophenyl)-1-(4-fluorophenyl)-3-(1H-indol-3-yl)-7,7-dimethyl-7,8-dihydro-1H-pyrazolo[3,4-b]quinolin-5(6H)-one (**7b**). The title compound was prepared according to General Procedure B using 1-(4-fluorophenyl)-3-(1H-indol-3-yl)-1H-pyrazol-5-amine **3c** (300 mg, 1.02 mmol), dimedone (143 mg, 1.02 mmol) and 2,4-dichloro benzaldehyde (179 mg, 1.02 mmol) in acetic acid to yield **7b** (406 mg, 70%); yellow solid; mp 239-241 °C; ^{1}H NMR (400 MHz, $CDCl_3$): δ = 8.46-8.42 (m, 2H), 8.04 (s, 1H), 7.79 (d, 1H, J = 7.9 Hz), 7.33-7.19 (m, 5H, overlapped $CDCl_3$ residual signal), 7.12 (t, 1H, J = 7.7 Hz), 6.87-6.82 (m, 2H), 6.40 (d, 1H, J = 2.4 Hz), 3.28 (s, 2H), 2.61 (d, 1H J = 16.2 Hz), 2.49 (d, 1H J = 16.2 Hz), 1.178 (s, 3H), 1.171 (s, 3H) ppm; ^{13}C NMR (75 MHz, DMSO-d_6): δ = 196.5, 163.5, 160.1 ($J_{C\text{-}F}$ = 245.0 Hz), 149.9, 143.4, 142.8, 135.5, 135.1, 135.0, 134.9, 133.1, 132.2, 130.8, 128.0, 126.6, 126.3, 125.6, 123.0, 122.9, 121.7, 120.2 ($J_{C\text{-}F}$ = 5.8 Hz), 119.5, 116.0 ($J_{C\text{-}F}$ = 22.7 Hz), 114.1, 111.4, 106.0, 52.8, 47.5, 31.9, 27.9, 27.2 ppm; FT-IR (KBr, ν_{max}/cm-1) 3435, 2143, 771, 672; HRMS (ESI): *m/z* calcd for $C_{32}H_{23}Cl_2FN_4O$ $[M + H]^+$ 569.1311, found 569.1306.

1,4-Bis(4-chlorophenyl)-3-(1H-indol-3-yl)-7,7-dimethyl-7,8-dihydro-1H-pyrazolo[3,4-b]quinolin-5(6H)-one (**7c**). The title compound was prepared according to General Procedure C using **6a** (300 mg, 0.54 mmol) and DDQ (123 mg, 0.54 mmol) in acetonitrile to yield **7c** (223 mg, 75%) ; yellow solid; mp 220-222 °C; ^{1}H NMR (400 MHz, $CDCl_3$): δ = 8.48 (d, 2H, J = 8.9 Hz), 8.01 (d, 2H, J = 7.6 Hz), 7.52 (d, 2H, J = 8.8 Hz), 7.32 (d, 1H, J = 8.0 Hz), 7.23 (t, 1H, J = 7.0 Hz), 7.19-7.15 (m, 3H), 7.04 (d, 2H, J = 8.3 Hz), 5.94 (d, 1H, J = 2.7 Hz), 3.28 (s, 2H), 2.55 (s, 2H), 1.17 (s, 6H) ppm. ^{13}C NMR (75 MHz, DMSO-d_6): δ = 196.7, 163.3, 149.8, 147.0, 143.2, 137.6, 135.7, 135.5, 132.5, 130.1, 129.1, 127.4, 126.5, 126.0, 122.0, 121.7, 120.5, 119.7, 114.4, 111.4, 106.1, 53.4, 47.7, 32.0, 29.0, 27.6 ppm; FT-IR (KBr, ν_{max}/cm-1) 3398, 3020, 1556, 1088, 763, 669; HRMS (ESI): *m/z* calcd for $C_{32}H_{24}Cl_2N_4O$ $[M + H]^+$ 551.1405; found: 551.1398.

4-(4-Chlorophenyl)-1-(4-fluorophenyl)-3-(1H-indol-3-yl)-7,7-dimethyl-7,8-dihydro-1H-pyrazolo[3,4-b]quinolin-5(6H)-one (**7d**). The title compound was prepared according to General Procedure C using **6b** (300 mg, 0.55 mmol) and DDQ (126 mg, 0.55 mmol) in acetonitrile to yield **7d** (211 mg, 75%); yellow solid; mp 182-184 °C; ^{1}H NMR (400 MHz, $CDCl_3$): δ = 8.46-8.43 (m, 2H), 8.0 (d, 2H, J = 8.0 Hz), 7.32 (d, 1H, J = 8.0 Hz), 7.27-7.20 (m, 3H), 7.18-7.14 (m, 3H), 7.05 (d, 2H, J = 8.4 Hz), 5.95 (d, 1H, J = 2.6 Hz), 3.28 (s, 2H), 2.55 (s, 2H), 1.17 (s, 6H) ppm; ^{13}C NMR (75 MHz, DMSO-d_6): δ = 196.7, 163.3, 160.1 ($J_{C\text{-}F}$ = 241.7 Hz), 147.0, 142.9, 135.8, 135.5, 135.2, 135.1, 132.5, 130.0, 127.4, 126.3, 126.1, 122.8 ($J_{C\text{-}F}$ = 8.2 Hz), 121.6, 120.5, 120.4, 119.6, 115.9 ($J_{C\text{-}F}$ = 22.7 Hz), 114.1, 111.3, 106.2, 53.4, 47.7, 31.9, 27.6 ppm; FT-IR (KBr, vmax/cm-1) 3398, 3020, 1215, 1087, 760, 669; HRMS (ESI): m/z calcd for $C_{32}H_{24}ClFN_4O$ $[M + H]^+$ 535.1701, found 535.1695.

*1-(4-Chlorophenyl)-3-(1H-indol-3-yl)-4-(4-methoxyphenyl)-7,7-dimethyl-7,8-dihydro-1H-pyrazolo[3,4-b]quinolin-5(6H)-one (**7e**).* The title compound was prepared according to General

Procedure B using 1-(4-chlorophenyl)-3-(1H-indol-3-yl)-1H-pyrazol-5-amine **3a** (300 mg, 0.97 mmol), dimedone (136 mg, 0.97 mmol) and 4-methoxy benzaldehyde (132 mg, 0.97 mmol) in acetic acid to yield **7e** (403 mg, 76%); yellow solid; mp 190-192 °C; ^{1}H NMR (400 MHz, $CDCl_3$): δ = 8.51-8.48 (m, 2H), 8.16-8.14 (m, 1H), 7.95 (s, 1H), 7.54-7.50 (m, 2H), 7.32-7.30 (m, 1H), 7.24-7.17 (m, 2H), 7.06 (d, 2H, J = 8.6 Hz), 6.78 (d, 2H, J = 8.6 Hz), 5.86 (d, 1H, J = 2.7 Hz), 3.81 (s, 3H), 3.27 (s, 2H), 2.56 (s, 2H), 1.17 (s, 6H) ppm. ^{13}C NMR (100 MHz, $CDCl_3$): δ = 197.9, 163.4, 159.5, 150.6, 149.1, 143.4, 138.1, 135.5, 131.3, 129.9, 129.5, 129.2, 126.6, 126.2, 122.7, 122.3, 121.4, 120.9, 120.8, 115.6, 113.4, 110.9, 108.2, 55.5, 54.6, 48.8, 32.5, 28.4 ppm; FT-IR (KBr, ν_{max}/cm^{-1}) 3468, 3019, 2962, 1034, 928, 770, 669; HRMS (ESI): *m/z* calcd for $C_{33}H_{27}ClN_4O_2$ $[M + H]^+$ 547.1901; found: 547.1885.

*1-(4-Chlorophenyl)-4-(2,5-dimethoxyphenyl)-3-(1H-indol-3-yl)-7,7-dimethyl-7,8-dihydro-1H-pyrazolo[3,4-b]quinolin-5(6H)-one (**7f**).* The title compound was prepared according to General Procedure B using 1-(4-chlorophenyl)-3-(1H-indol-3-yl)-1H-pyrazol-5-amine **3a** (300 mg, 0.97 mmol), dimedone (136 mg, 0.97 mmol) and 2,5-dimethoxy benzaldehyde (161 mg, 0.97 mmol) in acetic acid to yield **7f** (415 mg, 74%); yellow solid; mp >270 °C; ^{1}H NMR (300 MHz, DMSO-d_6): δ = 8.49 (d, 2H, J = 8.8 Hz), 8.0 (d, 1H, J = 7.8 Hz), 7.93 (s, 1H), 7.51 (d, 2H, J = 8.8 Hz), 7.30 (d, 1H, J = 7.9 Hz), 7.21-7.12 (m, 2H), 6.77 (dd, 1H, J = 9.0, 2.9 Hz), 6.67 (d, 1H, J = 8.9 Hz), 6.46 (d, 1H, J = 2.8 Hz), 6.09 (d, 1H, J = 2.4 Hz), 3.39 (s, 3H), 3.36 (s, 3H), 3.26 (s, 2H), 2.58 (d, 1H, J = 16.1 Hz), 2.51 (d, 1H, J = 16.0 Hz), 1.17 (s, 6H) ppm; ^{13}C NMR (75 MHz, DMSO-d_6) δ = 196.3, 162.8, 152.9, 150.0, 144.7, 143.5, 137.7, 135.4, 129.9, 129.1, 126.5, 126.3, 126.1, 122.0, 121.5, 121.3, 120.3, 119.6, 115.3, 114.5, 114.1, 111.9, 111.2, 106.1, 55.6, 55.2, 53.1, 47.6, 31.8, 28.0, 27.3 ppm; FT-IR (KBr, ν_{max}/cm^{-1}) 3435, 2917, 2143, 826, 772; HRMS (ESI): *m/z* calcd for $C_{34}H_{29}ClN_4O_3$ $[M + H]^+$ 577.2006, found 577.2004.

*1-(4-Chlorophenyl)-3-(1H-indol-3-yl)-7,7-dimethyl-4-(2,3,4-trimethoxyphenyl)-7,8-dihydro-1H-pyrazolo[3,4-b]quinolin-5(6H)-one (**7g**).* The title compound was prepared according to General Procedure B using 1-(4-chlorophenyl)-3-(1H-indol-3-yl)-1H-pyrazol-5-amine **3a** (300 mg, 0.97 mmol), dimedone (136 mg, 0.97 mmol) and 2,3,4-trimethoxy benzaldehyde (190 mg, 0.97 mmol) in acetic acid to yield **7g** (441 mg, 75%); yellow solid; mp 185-188 °C; ^{1}H NMR (400 MHz, $CDCl_3$): δ = 8.50 (d, 2H, J = 8.6 Hz), 8.13 (d, 1H, J = 6.7 Hz), 8.04 (s, 1H), 7.52 (d, 2H, J = 8.6 Hz), 7.29 (d, 2H, J = 7.4 Hz), 7.21-7.17 (m, 2H), 6.64 (d, 1H, J = 8.4 Hz), 6.49 (d, 1H, J = 8.4 Hz), 6.08 (s, 1H), 3.85 (s, 3H), 3.70 (s, 3H), 3.49 (s, 3H), 3.26 (s, 2H), 2.55 (s, 2H), 1.17 (s, 6H); ^{13}C NMR (75 MHz, DMSO-d_6): δ = 196.7, 163.0, 153.8, 150.1, 149.8, 144.9, 143.7, 141.5, 137.7, 135.6, 129.9, 129.1, 126.4, 126.1, 123.8, 123.1, 121.9, 121.6, 121.2, 120.7, 119.8, 115.0, 111.3, 107.5, 106.3, 60.2, 59.8, 56.0, 53.4, 47.6, 31.9, 28.2, 27.1 ppm; FT-IR (KBr, ν_{max}/cm^{-1}) 3366, 3018, 2956, 1095, 762, 669; HRMS (ESI): *m/z* calcd for $C_{35}H_{31}ClN_4O_4$ $[M + H]^+$ 607.2112, found 607.2102.

*4-(2,5-Dimethoxyphenyl)-1-(4-fluorophenyl)-3-(1H-indol-3-yl)-7,7-dimethyl-7,8-dihydro-1H-pyrazolo[3,4-b]quinolin-5(6H)-one (**7h**).* The title compound was prepared according to General Procedure B using 1-(4-fluorophenyl)-3-(1H-indol-3-yl)-1H-pyrazol-5-amine **3c** (300 mg, 1.02 mmol), dimedone (143 mg, 1.02 mmol) and 2,5-dimethoxy benzaldehyde (170 mg, 1.02 mmol) in acetic acid to yield **7h** (416 mg, 73%); yellow solid; mp 130-132 °C; ^{1}H NMR (300 MHz, DMSO-d_6): δ = 11.09 (s, 1H), 8.38 (br d, 2H, J = 2.7 Hz), 7.97 (d, 1H, J = 7.2 Hz), 7.50-7.45 (t, 2H, J = 8.1 Hz), 7.33 (d, 1H, J = 7.8 Hz), 7.10-7.04 (m, 2H), 6.84-6.80 (m, 2H), 6.53 (s, 1H), 5.92 (s, 1H), 3.44 (s, 3H), 3.31 (s, 3H, overlapped with H_2O residual signal), 3.21 (s, 2H), 2.49 (s, 2H, overlapped with DMSO-d_6 residual signal), 1.10 (s, 3H), 1.08 (s, 3H) ppm; ^{13}C NMR (75 MHz, DMSO-d_6): δ = 196.3, 162.8, 160.0 ($J_{C\text{-}F}$ = 234.4 Hz), 152.9, 150.0, 149.8, 144.7, 143.2,

135.4, 135.29, 135.26, 126.6, 126.2, 122.8 ($J_{C\text{-}F}$ = 8.3 Hz), 121.5, 121.2, 120.3, 119.6, 115.9 ($J_{C\text{-}F}$ = 22.5 Hz), 115.2, 114.2, 114.1, 111.9, 111.2, 106.2, 55.6, 55.2, 53.1, 47.6, 31.9, 28.0, 27.3 ppm; ppm; FT-IR (KBr, ν_{max}/cm^{-1}) 3436, 2143, 772, 673; HRMS (ESI): *m/z* calcd for $C_{34}H_{29}FN_4O_3$ [M + H]$^+$ 561.2302, found 561.2300.

*1-(3,4-Dichlorophenyl)-4-(3,4-dimethoxyphenyl)-3-(1H-indol-3-yl)-7,7-dimethyl-7,8-dihydro-1H-pyrazolo[3,4-b]quinolin-5(6H)-one (**7i**).* The title compound was prepared according to General Procedure C using **6e** (300 mg, 0.48 mmol) and DDQ (111 mg, 0.48 mmol) in acetonitrile to yield **7i** (228 mg, 75%); yellow solid; mp 158-159 °C; ^{1}H NMR (400 MHz, $CDCl_3$): δ = 8.78 (d, 1H, *J* = 2.4 Hz), 8.47 (dd, 1H, *J* = 8.8, 2.5 Hz), 8.07-8.05 (m, 2H), 7.60 (d, 1H, *J* = 8.8 Hz), 7.33-7.31 (m, 1H), 7.24-7.17 (m, 2H), 6.79 (d, 1H, *J* = 8.2 Hz), 6.72 (dd, 1H, *J* = 8.2, 1.9 Hz), 6.55 (d, 1H, *J* = 1.8 Hz), 5.92 (d, 1H, *J* = 2.7 Hz), 3.90 (s, 3H), 3.33 (s, 3H), 3.29 (s, 2H), 2.62 (d, 1H, *J* = 13.8 Hz), 2.54 (d, 1H, *J* = 15.0 Hz), 1.25 (s, 6H) ppm; ^{13}C NMR (100 MHz, DMSO-d_6) δ = 196.6, 163.2, 149.9, 148.8, 148.3, 148.1, 144.0, 138.5, 135.4, 131.4, 131.0, 128.8, 127.4, 127.0, 125.9, 125.5, 121.2, 121.0, 120.4, 119.7, 114.8, 113.2, 111.3, 106.0, 55.6, 55.2, 53.6, 47.7, 32.0, 27.8, 27.5 ppm; FT-IR (KBr, ν_{max}/cm^{-1}) 3372, 3020, 1028, 760, 669; HRMS (ESI): *m/z* calcd for $C_{34}H_{28}Cl_2N_4O_3$ [M + H]$^+$ 611.1617, found. 611.1602.

*1-(4-Chlorophenyl)-3-(1H-indol-3-yl)-7,7-dimethyl-4-(3,4,5-trimethoxyphenyl)-7,8-dihydro-1H-pyrazolo[3,4-b]quinolin-5(6H)-one (**7j**).* The title compound was prepared according to General Procedure C using **6c** (300 mg, 0.49 mmol) and DDQ (111 mg, 0.49 mmol) in acetonitrile to yield **7j** (223 mg, 75%); yellow solid; mp 256-258 °C; ^{1}H NMR (300 MHz, DMSO-d_6): δ = 11.13 (s, 1H), 8.46-8.42 (m, 2H), 7.84 (d, 1H, *J* = 7.8 Hz), 7.72-7.67 (m, 2H), 7.34 (d, 1H, *J* = 8.1 Hz), 7.13-7.07 (m, 1H), 7.04-6.99 (m, 1H), 6.38 (s, 2H), 6.21 (d, 1H, *J* = 2.7 Hz), 3.67 (s, 3H), 3.38 (s, 6H), 3.24 (s, 2H), 2.57 (s, 2H), 1.10 (s, 6H); ^{13}C NMR (100 MHz, DMSO-d_6) δ =

196.5, 163.2, 152.2, 149.8, 148.3, 143.5, 137.7, 137.4, 135.4, 131.5, 130.0, 129.1, 126.2, 126.1, 122.1, 121.4, 120.8, 120.1, 119.4, 114.8, 111.2, 106.6, 106.5, 60.1, 55.6, 53.6, 47.8, 32.1, 27.7 ppm; FT-IR (KBr, v_{max}/cm^{-1}) 3365, 3019, 760, 669; HRMS (ESI): *m/z* calcd for $C_{35}H_{31}ClN_4O_4$ $[M + H]^+$ 607.2112, found 607.2098.

*1-(3,4-Dichlorophenyl)-4-(2,5-dimethoxyphenyl)-3-(1H-indol-3-yl)-7,7-dimethyl-7,8-dihydro-1H-pyrazolo[3,4-b]quinolin-5(6H)-one (**7k**).* The title compound was prepared according to General Procedure C using **6d** (300 mg, 0.48 mmol) and DDQ (111 mg, 0.48 mmol) in acetonitrile to yield **7k** (211 mg, 72%); yellow solid; mp 268-270 °C; ^{1}H NMR (300 MHz, DMSO-d_6): δ = 11.14 (s, 1H), 8.76 (d, 1H, *J* = 2.4 Hz), 8.46 (dd, 1H, *J* = 8.7, 2.4 Hz), 7.96 (d, 1H, *J* = 7.5 Hz), 7.90 (d, 1H, *J* = 8.7 Hz), 7.34 (d, 1H, *J* = 7.5 Hz), 7.15-7.04 (m, 2H), 6.89-6.80 (m, 2H), 6.54 (d, 1H, *J* = 2.7 Hz), 5.95 (d, 1H, *J* = 2.7 Hz), 3.45 (s, 3H), 3.30 (s, 3H), 3.26 (s, 2H), 2.53 (s, 2H, overlapped with DMSO-d_6 residual signal), 1.12 (s, 3H), 1.09 (s, 3H) ppm; ^{13}C NMR (75 MHz, DMSO-d_6): δ = 196.8, 163.5, 153.4, 150.7, 150.4, 145.3, 144.5, 139.1, 135.9, 132.0, 131.7, 128.1, 126.9, 126.8, 126.5, 122.1, 121.8, 120.7, 120.6, 120.2, 115.8, 115.3, 114.7, 112.5, 111.8, 106.4, 56.1, 55.7, 53.5, 48.0, 32.4, 28.4, 27.8 ppm; FT-IR (KBr, v_{max}/cm^{-1}) 3435, 2918, 1219, 771, 673; HRMS (ESI): *m/z* calcd for $C_{34}H_{28}Cl_2N_4O_3$ $[M + H]^+$ 611.1617, found 611.1610.

*1-(4-Chlorophenyl)-4-(2,5-dimethoxyphenyl)-3-(1H-indol-3-yl)-6,7-dihydrocyclopenta[e]pyrazolo[3,4-b]pyridin-5(1H)-one (**7l**).* The title compound was prepared according to General Procedure C using **6g** (300 mg, 0.55 mmol) and DDQ (126 mg, 0.55 mmol) in acetonitrile to yield **7l** (217 mg, 74%); yellow solid; mp 234-236 °C; ^{1}H NMR (400 MHz, $CDCl_3$): δ = 8.48-8.44 (m, 2H), 8.11 (d, 1H, *J* = 7.3 Hz), 7.97 (s, 1H), 7.55-7.52 (m, 2H), 7.31 (dd, 1H, *J* = 6.8, 1.0 Hz), 7.23-7.15 (m, 2H), 6.87 (dd, 1H, *J* = 9.0, 3.1 Hz), 6.69 (d, 1H, *J* = 9.1

Hz), 6.65 (d, 1H, *J* = 3.1 Hz), 6.19 (d, 1H, *J* = 2.6 Hz), 3.49 (s, 3H), 3.40-3.37 (m, 2H), 3.29 (s, 3H), 2.85-2.81 (m, 2H) ppm. ^{13}C NMR (75 MHz, DMSO-d_6): δ = 201.7, 174.6, 152.7, 152.4, 150.6, 144.1, 142.3, 137.6, 135.5, 130.0, 129.1, 126.3, 125.9, 122.7, 122.5, 122.2, 121.6, 120.5, 119.7, 115.9, 115.6, 114.7, 112.1, 111.3, 106.1, 55.5, 55.4, 36.5, 27.7 ppm; FT-IR (KBr, ν_{max}/cm^{-1}) 3398, 3019, 2925, 758, 668; HRMS (ESI): m/z calcd for $C_{31}H_{23}ClN_4O_3$ $[M + H]^+$ 535.1537; found: 535.1546.

*1-(4-Chlorophenyl)-3-(1H-indol-3-yl)-4-(3,4,5-trimethoxyphenyl)-6,7-dihydrocyclopenta[e]pyrazolo[3,4-b]pyridin-5(1H)-one (**7m**).* The title compound was prepared according to General Procedure C using **6h** (300 mg, 0.52 mmol) and DDQ (120 mg, 0.52 mmol) in acetonitrile to yield **7m** (205 mg, 70%); yellow solid; mp >270 °C; ^{1}H NMR (400 MHz, $CDCl_3$): δ = 8.46 (d, 2H, *J* = 8.9 Hz), 8.19 (s, 1H), 8.03 (d, 1H, *J* = 7.7 Hz), 7.54 (d, 2H, *J* = 8.8 Hz), 7.33 (d, 1H, *J* = 7.9 Hz), 7.23-7.14 (m, 2H), 6.50 (s, 2H), 6.17 (d, 1H, *J* = 2.6 Hz), 3.86 (s, 3H), 3.46 (s, 6H), 3.42-3.39 (m, 2H), 2.89-2.86 (m, 2H) ppm. ^{13}C NMR (75 MHz, $CDCl_3$ + DMSO-d_6): δ = 202.2, 174.6, 152.9, 151.9, 146.4, 143.7, 138.2, 137.5, 135.5, 131.0, 128.7, 126.8, 125.9, 125.8, 122.3, 121.7, 121.5, 120.0, 119.8, 114.7, 111.1, 107.6, 106.9, 60.5, 55.4, 36.7, 27.9 ppm; FT-IR (KBr, ν_{max}/cm^{-1}) 3388, 3019, 2927, 758, 669; HRMS (ESI): *m/z* calcd for $C_{32}H_{25}ClN_4O_4$ $[M + H]^+$ 565.1643; found: 565.1651.

*1-(3,4-Dichlorophenyl)-4-(3,4-dimethoxyphenyl)-3-(1H-indol-3-yl)-6,7-dihydrocyclopenta[e]pyrazolo[3,4-b]pyridin-5(1H)-one (**7n**).* The title compound was prepared according to General Procedure C using **6j** (300 mg, 0.52 mmol) and DDQ (119 mg, 0.52 mmol) in acetonitrile to yield **7n** (201 mg, 68%); yellow solid; mp 270-272 °C; ^{1}H NMR (400 MHz, DMSO-d_6): δ = 11.24 (s, 1H), 8.74 (d, 1H, *J* = 2.4 Hz), 8.44 (dd, 1H, *J* = 8.9, 2.5 Hz), 8.05 (d, 1H, *J* = 7.7 Hz), 7.89 (d, 1H, *J* =8.9 Hz), 7.35 (d, 1H, *J* = 7.8 Hz), 7.16-7.07 (m, 2H), 6.89-6.84

(m, 2H), 6.82 (s, 1H), 5.99 (d, 1H, J = 2.6 Hz), 3.81 (s, 3H), 3.34 (s, 3H, overlapped with residual H_2O signal), 2.77 (br s, 2H), 2.50 (s, 2H, overlapped with DMSO-d_6 residual signal) ppm. ^{13}C NMR (75 MHz, $CDCl_3$ + DMSO-d_6): δ = 202.07, 174.60, 152.87, 149.23, 147.47, 146.38, 143.93, 138.16, 135.20, 132.22, 130.10, 128.67, 126.34, 125.56, 123.91, 122.65, 122.01, 121.68, 121.61, 120.05, 119.86, 119.70, 114.73, 113.19, 110.85, 109.90, 106.44, 55.39, 54.92, 36.55, 27.71 ppm; FT-IR (KBr, ν_{max}/cm^{-1}) 3435, 3019, 770, 669, 625; HRMS (ESI): *m/z* calcd for $C_{31}H_{22}Cl_2N_4O_3$ $[M + H]^+$ 569.1147; found: 569.1128.

*1-(4-Chlorophenyl)-3-(1H-indol-3-yl)-4-(4-methoxyphenyl)indeno[2,1-e]pyrazolo[3,4-b]pyridin-5(1H)-one (**7o**).* The title compound was prepared according to General Procedure B using 1-(4-chlorophenyl)-3-(1H-indol-3-yl)-1H-pyrazol-5-amine **3a** (300 mg, 0.97 mmol), 1,3-indanedione (142 mg, 0.97 mmol) and 4-methoxy benzaldehyde (132 mg, 0.97 mmol) in acetic acid to yield **7o** (380 mg, 71%); yellow solid; mp >270 °C; ^{1}H NMR (300 MHz, DMSO-d_6): δ = 11.16 (s, 1H), 8.45 (d, 2H, J = 9.0 Hz), 8.08 (d, 1H, J = 7.5 Hz), 7.93 (d, 1H, J = 7.5 Hz), 7.70-7.63 (m, 3H), 7.52 (d, 2H, 5.7 Hz), 7.33 (d, 1H, J = 7.8 Hz), 7.23 (d, 2H, J = 8.7 Hz), 7.15-7.04 (m, 2H), 6.80 (d, 2H, J = 8.4 Hz), 5.83 (d, 1H, J = 2.4 Hz), 3.80 (s, 3H) ppm. ^{13}C NMR (75 MHz, DMSO-d_6): δ = 188.5, 164.0, 159.9, 151.9, 145.9, 144.1, 141.0, 137.4, 136.5, 135.5, 134.8, 131.6, 130.9, 130.0, 128.9, 127.2, 125.7, 124.2, 122.8, 122.0, 121.5, 120.9, 120.8, 119.7, 119.4, 113.8, 112.8, 111.2, 105.9, 55.1 ppm; FT-IR (KBr, ν_{max}/cm^{-1}) 3436, 2143, 772, 673; HRMS (ESI): *m/z* calcd for $C_{34}H_{21}ClN_4O_2$ $[M + H]^+$ 553.1431; found: 553.1430.

*1-(4-Chlorophenyl)-4-(2,5-dimethoxyphenyl)-3-(1H-indol-3-yl)indeno[2,1-e]pyrazolo[3,4-b]pyridin-5(1H)-one (**7p**).* The title compound was prepared according to General Procedure B using 1-(4-chlorophenyl)-3-(1H-indol-3-yl)-1H-pyrazol-5-amine **3a** (300 mg, 0.97 mmol), 1,3-indanedione (142 mg, 0.97 mmol) and 2,5-dimethoxy benzaldehyde (161 mg, 0.97 mmol) in

acetic acid to yield **7p** (418 mg, 74%); yellow solid; mp 240-242 °C; ^{1}H NMR (300 MHz, DMSO-d_6): δ = 11.15 (s, 1H), 8.49 (d, 2H, J = 8.1 Hz), 8.04 (d, 2H, J = 6.6 Hz), 7.76-7.70 (m, 3H), 7.62-7.58 (m, 2H), 7.34 (d, 1H, J = 7.5 Hz), 7.13-6.99 (m, 3H), 6.87 (br s, 2H), 6.10 (s, 1H), 3.57 (s, 3H), 3.20 (s, 3H) ppm. ^{13}C NMR (75 MHz, DMSO-d_6): δ = 188.5, 164.1, 152.7, 152.0, 150.6, 144.5, 142.3, 141.2, 137.5, 136.7, 135.5, 135.1, 131.9, 130.3, 129.1, 126.1, 125.9, 123.2, 122.5, 122.1, 121.6, 121.2, 120.4, 119.7, 115.9, 115.8, 114.5, 112.1, 111.3, 106.0, 55.5 ppm; FT-IR (KBr, v_{max}/cm^{-1}) 3434, 1637, 770, 671; HRMS (ESI): *m/z* calcd for $C_{35}H_{23}ClN_4O_3$ $[M + H]^+$ 583.1537; found: 583.1530.

*1-(4-Chlorophenyl)-3-(1H-indol-3-yl)-4-(3,4,5-trimethoxyphenyl)indeno[2,1-e]pyrazolo[3,4-b]pyridin-5(1H)-one (**7q**).* The title compound was prepared according to General Procedure B using 1-(4-chlorophenyl)-3-(1H-indol-3-yl)-1H-pyrazol-5-amine **3a** (300 mg, 0.97 mmol), 1,3-indanedione (142 mg, 0.97 mmol) and 3,4,5-trimethoxy benzaldehyde (190 mg, 0.97 mmol) in acetic acid to yield **7q** (457 mg, 77%); yellow solid; mp 174-176 °C; ^{1}H NMR (300 MHz, DMSO-d_6): δ = 11.21 (s, 1H), 8.47 (d, 2H, J = 9.0 Hz), 8.01 (d, 1H, J = 7.5 Hz), 7.85 (d, 1H, J = 7.8 Hz), 7.73-7.70 (m, 3H), 7.64-7.54 (m, 2H), 7.35 (d, 1H, J = 7.8 Hz), 7.13-6.99 (m, 2H), 6.62 (s, 2H), 6.30 (d, 1H, J = 2.7 Hz), 3.67 (s, 3H), 3.38 (s, 6H) ppm. ^{13}C NMR (100 MHz, $CDCl_3$ + DMSO-d_6): δ = 188.8, 164.4, 152.1, 151.6, 145.8, 143.7, 141.3, 138.0, 137.2, 136.6, 135.1, 134.2, 131.0, 130.7, 128.4, 126.1, 125.6, 122.7, 121.9, 121.2, 120.7, 119.6, 119.3, 119.2, 114.0, 110.8, 107.1, 106.4, 60.1, 55.1 ppm; FT-IR (KBr, v_{max}/cm^{-1}) 3435, 2089, 1634, 1501, 1337, 1219, 1118, 772, 673; HRMS (ESI): *m/z* calcd for $C_{36}H_{25}ClN_4O_4$ $[M + H]^+$ 613.1643; found: 613.1637.

*4-(2,5-Dimethoxyphenyl)-1-(4-fluorophenyl)-3-(1H-indol-3-yl)indeno[2,1-e]pyrazolo[3,4-b]pyridin-5(1H)-one (**7r**).* The title compound was prepared according to General Procedure B

using 1-(4-fluorophenyl)-3-(1H-indol-3-yl)-1H-pyrazol-5-amine **3c** (300 mg, 1.02 mmol), 1,3-indanedione (150 mg, 1.02 mmol) and 2,5-dimethoxy benzaldehyde (170 mg, 1.02 mmol) in acetic acid to yield **7r** (416 mg, 72%); red solid; mp >270 °C; ^{1}H NMR (300 MHz, DMSO-d_6): δ = 11.14 (s, 1H), 8.47-8.42 (m, 2H), 8.06-8.01 (m, 2H), 7.79-7.74 (m, 1H), 7.65-7.48 (m, 4H), 7.34 (d, 1H, J = 9 Hz), 7.15-6.98 (m, 3H), 6.88-6.86 (m, 2H), 6.10 (s, 1H), 3.57 (s, 3H), 3.22 (s, 3H) ppm. ^{13}C NMR (75 MHz, DMSO-d_6): δ = 188.6, 164.1, 160.2 ($J_{C\text{-}F}$ = 242.4 Hz), 152.7, 151.9, 150.6, 144.3, 142.4, 141.3, 136.8, 135.5, 135.2, 135.1, 135.0, 132.0, 126.0 ($J_{C\text{-}F}$ = 9.3 Hz), 123.4, 123.3, 123.2, 122.2, 121.6, 121.2, 120.5, 120.3, 119.7, 116.0 ($J_{C\text{-}F}$ = 22.8 Hz), 115.8, 114.3, 112.1, 111.3, 106.1, 55.5, 55.4 ppm; FT-IR (KBr, ν_{max}/cm^{-1}) 3436, 2143, 772, 673; HRMS (ESI): *m/z* calcd for $C_{35}H_{23}FN_4O_3$ $[M + H]^+$ 567.1832; found: 567.1803.

*1-(4-Chlorophenyl)-3-(1H-indol-3-yl)-4-(2,3,4-trimethoxyphenyl)indeno[2,1-e]pyrazolo[3,4-b]pyridin-5(1H)-one (**7s**)*. The title compound was prepared according to General Procedure C using **6o** (300 mg, 0.48 mmol) and DDQ (110 mg, 0.48 mmol) in acetonitrile to yield **7s** (220 mg, 75%); yellow solid; mp 245-248 °C; ^{1}H NMR (300 MHz, DMSO-d_6): δ = 11.25 (br s, 1H), 8.49 (d, 2H, J = 8.0 Hz), 8.17 (d, 1H, J = 6.6 Hz), 8.02 (d, 1H, J = 6.8 Hz), 7.74-7.56 (m, 5H), 7.35 (d, 1H, J = 6.8 Hz), 7.12 (s, 2H), 6.98 (d, 1H, J = 8.2 Hz), 6.81 (d, 1H, J = 8.2 Hz), 5.97 (s, 1H) 3.90 (s, 3H) 3.55 (s, 3H), 3.34 (s, 3H, overlapped with residual H_2O signal) ppm; 13C NMR (75 MHz, DMSO-d_6): δ = 188.9, 164.1, 154.7, 152.0, 150.7, 144.6, 142.6, 141.4, 141.3, 137.5, 136.8, 135.6, 135.3, 132.1, 130.4, 129.3, 126.4, 125.9, 124.4, 123.3, 122.6, 121.8, 121.3, 120.9, 120.69, 119.9, 119.7, 114.9, 111.4, 107.5, 106.2, 60.4, 60.3, 56.1 ppm; HRMS (ESI): *m/z* calcd for $C_{36}H_{25}ClN_4O_4$ $[M + H]^+$ 613.1643; found: 613.1631.

Parasite, Cell Culture and Infection. Promastigotes of *L. donovani* strain (MHOM/IN/80/Dd8) transfected with luciferase gene[23] were cultured in M199 medium supplemented with 10% heat

inactivated fetal bovine serum (FBS) and G418 disulphate (20 μg/mL) at 24 °C. J774 macrophages and Vero cells were cultured in RPMI supplemented with 10% FBS, 100 U/mL penicillin, and 100 μg/mL streptomycin and incubated at 37 °C with 5% CO_2.

For *in vitro*, J774 macrophages were infected with *L. donovani* promastigotes in 1:10 ratio (cell:parasite) in 16 well chamber slides as described above. After 24 h of infection, **6j** and **6d** were added for 48 and 72 h (IC_{50} and MIC dose). Cells were fixed in CH_3OH and stained with 20% Giemsa stain. The inhibition of parasitic growth was determined by comparison of drug treated parasites/100 macrophages with that of untreated infected controls

Promastigotes Viability Assay by Luciferase and MTT Assay. To determine the antileishmanial activity of pyrazolodihydropyridines on *Leishmania* parasite, exponentially growing promastigotes (Dd8-Luc constitutively expressing firefly luciferase gene) seeded at 1×10^6 /mL/100 μl/well in 10% FBS enriched M199 medium in 96 well plates and were incubated with test compounds at two concentration (50 μM and 25 μM). Non-treated control parasites were also incubated with medium only also included in each plate. Miltefosine was added as a positive control and 0.1% DMSO was used as a vehicle control. After treatment for 72 h, Steady-Glo reagent (Promega) containing luciferin as substrate was added in 1:1 ratio and incubated for 1-2 min with gentle shaking to lyse the parasite suspension properly. Parasite multiplication expressed in terms of relative luminescence unit (RLU) was used to calculate the IC_{50} value of compounds by non-linear regression analysis of dose-response curve using the four-parameter Hill equations. IC_{50} was calculated for those compounds (**6j** and **6d**) which showed > 90 % inhibition of promastigotes.

To check antileishmanial activity against promastigotes, 1×10^6 log phase promastigotes were seeded into a 96-well plate, incubated for 12, 24, 48, and 72 h in the presence of **6j** and **6d** at

their respective IC_{50} concentrations and MIC. After incubation, the cells were centrifuged and the supernatant was aspirated. The cell pellet was washed with PBS (1X) twice and then finally suspended in 100 μL of PBS (1X) into a 96-well plate. Cell viability was assessed by MTT assay as described above.

Antiamastigote Assay. Briefly, J774 macrophages (4×10^4/mL/100 μL/well) were seeded in RPMI enriched with 10% FBS in 96 well plate and 16 - well chamber slide. After incubation for 24 h at 37 °C in a 5% CO_2, the medium was replaced with stationary phase luciferase expressing *L. donovani* promastigotes at a ratio of 1:8 (macrophages: parasites) and further incubated for 24 h. Compounds were serially diluted in fresh RPMI medium in two-fold concentration, with final assay concentrations ranging from 3.125-50 μM. After removal of non-internalized promastigotes by washing with complete RPMI medium, compounds were added to respective wells along with complete RPMI medium initially at 50 μM and 25 μM. Next, the plates were incubated for 72 h at 37 °C in 5% CO_2 incubator. On completion of incubation, medium from all wells was removed and 50 μL of phosphate buffer saline (PBS) was added along with a equal volume of Steady-Glo reagent (15 mg/mL). Further, reading was taken in a luminometer (Berthold) after gentle shaking for 1-2 min to lyse the cells. IC_{50} value of compounds **6j** and **6d** (showing > 90 % inhibition of amastigotes) was calculated by non-linear regression analysis of dose-response curve using the four-parameter Hill equations.

MIC (Maximal Inhibitory Concentration) Determination. To calculate MIC (maximal inhibitory concentration), extracellular promastigotes and intracellular amastigotes were treated with different concentration of compound 6d and 6j starting from 200 μM then serial half dilution upto 6 point for 72 hr. Parasite multiplication expressed in terms of relative

luminescence unit (RLU) was used to calculate the MIC value of compounds by non-linear regression analysis of dose-response curve using the four-parameter Hill equations.

Growth Curve Assay for Promastigote and Intracellular Amastigotes. The growth curve analysis for L. donovani promastigotes and intracellular amastigotes at various concentrations of **6j** and **6d** was performed using luciferase based assay. In brief, log phase promastigotes (1.0×106) were cultured in 96 well plates and subjected to various concentrations of 6j and 6d ranging from 200 to 6.25 μM by two fold serial dilution at optimal conditions (24 °C, pH 7.4). Growth curve was plotted by determination of relative luminescence units daily for up to 4 days in lysed promastigotes culture. Similarly, intracellular amastigotes were cultured at 37 °C with above-mentioned concentrations of **6d** and **6j** used for promastigotes. Growth of intracellular amastigotes in infected macrophages was also calculated by measurements of luciferase activity and expressed as RLU.

Mammalian Cell Cytotoxicity Assay. Vero cell line (derived from the kidney of African green monkey) and J774 macrophages were used to assess the cytotoxic effects of compounds. For the assay, 100 μL of cell suspension containing 1×10^5 cells were seeded onto each well of 96 well plates for 24 h. Compounds to be tested were serially diluted in two-fold for up to seven concentrations ranging from 500-7.81 μM. After incubation for 72 h, the cytotoxicity was assessed by MTT assay described previously with few modifications.[24] Briefly, 25 μL of stock MTT solution (5 mg/mL) prepared in phosphate buffer saline was added to each well and plates were incubated for 2h at 37 °C. At the end, medium containing MTT solution was removed and 100 μL of DMSO was added to solubilize the formazan crystals. The amount of formazan was measured at 540 nm on a microplate reader (Biotek Powerwave XS2) after gentle shaking of 15 min. The 50% cellular cytotoxic concentration (CC_{50}) of compounds was calculated as

previously described by Huber and Koella.[25] Selectivity index (SI) for compounds was calculated as the ratio of CC_{50} to the IC_{50} (inhibitory concentration against intracellular amastigotes).

Ethics Statement. The experiments were designed according to the Institute's Animal Ethical Committee (IAEC) of CSIR-CDRI and the whole study fulfilled the criteria of Committee for the Purpose of Control and Supervision of Experiments on Animals (CPCSEA), New Delhi, India. The experiments were performed in the most humane way possible giving minimum stress to the experimental animals (BALB/c mice). They were kept in a photoperiod of 12L:12D cycles (12 h of light and 12 h of dark) with relative humidity 60%, daytime light intensity of 300 Lux and supplied with ad libitum drinking water along with grain-supplemented standard rodent pellets.

Infection and Treatment of Animals. To establish the infection, an inoculum of *L. donovani* amastigotes was prepared from the spleen of 2 month-infected golden hamsters. Experimental BALB/c mice were then infected with 2×10^7 amastigotes suspended in PBS via a lateral tail vein. As liver or splenic biopsy were found to be fatal and increases the mortality of the infected animal, we routinely performed autopsy of randomly selected two Balb/c mice after 15 days of infection. For that, impression smears were prepared from the spleen/liver on glass slides, fixed in methanol and stained with 30% Giemsa stain in triple distilled water. In all occasions, we observed that splenic and liver parasitic burden lies between 5-10 amastigotes / 100 nucleated cells by counting parasites under bright field microscope. To study the dose kinetics of the compounds in mice, 5 mice per group were selected having grade I infection (5-10 amastigotes/100 nucleated cell). One group was taken as an infected untreated control, one as treated with a standard antileishmanial drug miltefosine and rest of the groups were selected to study the antileishmanial efficacy of **6d** and **6j** at a dose gradient ranging from 12.5 to 200

mg/kg. Miltefosine being water-soluble was dissolved in TDW and administered orally while the test compounds were dissolved in 8% DMSO in deionized water and administered intraperitoneally. Animals were treated with respective compounds via intraperitoneal route for five consecutive days. Animals were sacrificed at day 7 post-treatment to study the therapeutic efficacy of the compounds. Giemsa stained splenic and liver tissue smear was counted for amastigotes/1000 nucleated cells and was expressed as LDU.[26] For time kinetics studies of infection, BALB/c mice were infected for 15 days, followed by treatment with 50 mg/kg of 6j for 5 consecutive days as described above and were assessed for parasitic burden at various time points (1-7 wk) after treatment.

For a combinational study of **6j** with miltefosine, seven groups of mice were selected (5 mice/group). Group I served as normal control receiving vehicle (8% DMSO *i.p.*) only, group II served as infected untreated, group III receiving **6j** at a lower dose 25 mg/kg, group IV receiving **6j** at 50 mg/kg, group V as sub-curative miltefosine 5 mg/kg, group VI receiving combination of **6j** at 25 mg/kg along with miltefosine at 5mg/kg and group VII receiving curative dose of miltefosine 25 mg/kg. The respective doses were delivered for five consecutive days either orally or intraperitoneally for miltefosine **6j**, respectively. Mice from different experimental groups were sacrificed at day 4 and day 7 post treatments to study parasitic burden in spleen and liver and splenocytes were collected for various immunological assays.

Nitric Oxide (NO) Measurement by Griess Method and iNOS Expression by Real-Time PCR. To study the amount of nitric oxide released in the culture supernatant of murine splenocytes, the cells isolated at day 4 and day 7 post-treatment from various experimental groups and were cultured in Phenol Red-free complete RPMI 1640 and stimulated with 5 μg/mL SLA for 72 h at 37 °C in 5% CO_2 incubator. The supernatant was centrifuged at 1200 rpm for 10

min and was quantified for accumulated nitrite using Griess assay as described earlier. The absorbance at 540 nm was compared to a standard curve of serially diluted sodium nitrite to estimate the amount. For iNOS expression level, total RNA was extracted from splenocytes from different groups of mice using RNeasykit (Qiagen, USA). cDNA was synthesized using 1 μg of RNA as a templet using the Superscript first-strand synthesis system (Invitrogen, USA). Triplicate reactions were implemented using ABI Power SYBR Green PCR Master mix on Roche Applied Science light cycler 480.0, using software version 1.5.0. Primer sequences were as follows:

iNOS:	Forward	5′ CTTTGTGCGAAGTGTCAGTG 3′
	Reverse	5′ CACCTGGAACAGCACTCTCT 3′
β-Actin	Forward	5′ AAGAGCTATGAGCTGCCTGA 3′
	Reverse	5′ TACGGATGTCAACGTCACAC 3′

Relative quantification of iNOS was normalized to the housekeeping gene β-Actin mRNA level and expressed as a fold change compared with uninfected control using the comparative cycle threshold (CT) method.

T-Cell Proliferation Assay. To assess the T-cell proliferation of different experimental groups, splenocytes isolated at day 4 and day 7 post-treatment were suspended in Phenol Red-free complete RPMI 1640 after Ficoll density gradient centrifugation in numbers of 10^5/well as triplicates and stimulated either with 5 μg/mL SLA for 72 h at 37 °C in 5% CO_2 incubator. Cells were then treated with 0.5 mg/mL MTT solution in dark and the formazan formed were solubilized in DMSO. Optical density was read using ELISA reader at 540 nm (Powerwave XS2, Biotek Instruments, VT, USA).

Quantification of Th1/Th2 Cytokines by ELISA. To study the pro/anti-inflammatory cytokine synthesis, splenocytes (2×10^6) from different groups of mice were cultured in Phenol Red-free complete RPMI 1640 for 72 h along with 5 μg/mL of SLA. The supernatant was harvested and centrifuged at 1200 rpm for 10 minutes to remove cells and debris and was analyzed for released cytokines using sandwich ELISA kit (BD Biosciences) following the manufacturer's protocol. A standard curve with a cytokine-positive control was run in each assay and the lower limit of detection was determined to be 5.1, 2.5, 4, and 4.6 pg/mL for TNF-α, IL12p70, IL-10, and TGF-β, respectively.

Detection of Phosphatidylserine Externalization by Flow Cytometry. The percentage of promastigotes undergoing apoptosis was detected according to the manufacturer's protocol using Apoptosis Detection kit (Sigma-Aldrich, USA), with Annexin V-FITC and propidium iodide (PI). Binding of annexin V selectively to phosphatidylserine (PS) present on the outer cell membrane is a characteristic feature of apoptosis induction and PI labeling helps to distinguish between necrotic and apoptotic cell. In brief, 1×10^6 *L. donovani* promastigotes were treated with **6j** at IC_{50} and maximal inhibitory concentration (MIC *i.e.* 50 μM) obtained from promastigote susceptibility assay for 48 h. At the end of incubation, treated and non-treated promastigotes suspension were washed once with PBS and re-suspended in 1 X annexin binding buffer. Promastigotes were double stained with 5 μL of annexin V- FITC (50 μg/mL) and 10 μL of PI at 100 μg/mL, followed by incubation for 15 min at room temperature in the dark. Immediately after incubation, stained promastigotes were analyzed using FACS Calibur Flow Cytometer (Becton Dickinson, USA) with simultaneous monitoring of green fluorescence (515 nm) for annexin V- FITC and red fluorescence (623 nm) associated with PI and data was analyzed with Cell Quest software. Representative dot plots are divided into four quadrants. Lower right

quadrant belongs to apoptotic cells (annexin V^+/PI^-) and upper left quadrant belongs to necrotic cells (annexin V^-/ PI^+). Upper right quadrant belongs to late apoptotic (annexin V^+/ PI^+) and lower left quadrant shows survived cells.

JC-1 Staining for Mitochondrial Membrane Potential ($\Delta\Psi_m$) Measurement. For determination of MMP, untreated and treated *L. donovani* promastigotes were stained with JC-1(MitoProbe™ JC-1 Assay Kit, Molecular probes, USA). JC-1 (5′,6,6′-tetrachloro-1,1′,3,3′-tetraethylbenzimidazolylcarbocyanine iodide) is a cationic dye that exhibits potential-dependent accumulation in mitochondria, indicated by a fluorescence emission shift from green (~530 nm) to red (~590 nm). In healthy cells, JC-1 forms aggregate and emit red fluorescence; however after the loss of mitochondrial membrane potential, JC-1 forms monomer and emits green fluorescence. Briefly, 1×10^6 *L. donovani* promastigotes were treated with compound **6j** at 50 μM for 6 h, 12 h, 24 h and 48 h. At the end of incubation, cells were harvested, washed and re-suspended in 1X PBS. To the suspension, 10 μL of 200 μM (2 μM final concentration) JC-1 was added and incubated at 37 °C, 5% CO_2 for 30 min. The fluorescence intensity of samples was measured at 530 nm (green fluorescence representing cells with depolarized mitochondrial membrane potential) and 590 nm (red fluorescence denotes healthy population) in FACS Calibur Cytometer (Becton Dickinson, USA) and data was analyzed using Cell Quest Pro software.

***In Situ* Detection of DNA Fragmentation via TUNEL Assay.** *In situ* detection of cleaved, apoptotic DNA fragments of *L. donovani* promastigotes was performed using APO- BrdU TUNEL assay kit (Molecular Probes, USA) with slight modifications. In this assay, terminal deoxynucleotidyl transferase (TdT) binds to and adds 5- bromo-2′-deoxyuridine-5′-triphosphate (BrdUTP) to exposed 3′-OH ends of cleaved DNA fragments. After incorporation of BrdU into the DNA, labeled break sites are detected by using anti-BrdU monoclonal antibody conjugated

with Alexa Fluor 488. Briefly, 1×10^6 *L. donovani* promastigotes were incubated in the absence or presence of compound **6j** at IC_{50} and MIC (50 μM) for 48 h. At the end of incubation, treated and non-treated parasite suspension was washed once with 1X PBS and adhered onto poly-L-lysine coated slides and fixed with 1% para-formaldehyde. After that, promastigotes were permeabilized with ice-cold 70 % ethanol for 30 minutes on ice. Slides were then incubated in 50 μL of DNA labeling solution for 60 min at 37 °C followed by addition of propidium iodide / RNase A staining buffer. Further, slides were visualized under FLoid™ Cell Imaging Station, Life Technologies (California, USA).

Statistical Analysis. GraphPad Prism, version 5.0 was used to analyze and represent the data. The data shown are representative of a set of three independent experiments. The results are represented as mean ± SD. The differences between groups were analyzed by one-way ANOVA followed by Tukey's post-test and P value <0.05 between groups was considered as significant difference.

***In Vitro* Metabolic Stability.** Metabolic stability was performed in duplicate using glass tubes. To each tube, 457.5 μL of phosphate buffer (0.1 M, pH 7.4) and 12.5 μL of mice S9 fraction (20 mg/ml) was added and pre-incubated at 37 ± 0.2 °C for 5 min. Then 2.5 μL of test compound (1 mM) was added. For positive control testosterone was used as the test compound. The reaction was initiated by addition of 25 μL of NADPH (24 mM) and incubated for 0, 5, 10, 15, 30, 45 and 60 min. In the negative control, NADPH was replaced by 25 μL of phosphate buffer. Reaction was stopped by addition of 500 μL ice-cold acetonitrile followed by centrifugation for 15 min at 10,000 rpm. Supernatant was directly analyzed by HPLC. HPLC was run in an isocratic mode using methanol and triple distilled water as mobile phase in the ratio 80:20 (v/v) at a flow rate of

1 mL/min for both **6j** and **6d**. The compounds were separated on a Lichrosphere C18 column (4.6 mm × 250 mm, 5.0 μM).

Data Analysis. Percentage drug remaining was calculated using the following equation:

$$\% \text{ Drug remaining} = \frac{\text{Concentration of drug after incubation}}{\text{Concentration of drug before incubation}} \times 100$$

Non-linear regression analysis of the parent compound remaining against time was performed using Graph pad Prism software, version 5.0. The equation defining the regression analysis is as follows:

$$\% \text{ Parent drug remaining} = \text{Span}*e^{-kt} + \text{Plateau}$$

where 'Span' denotes the differences in the % parent drug remaining at time zero to time t, 'Plateau' is the % parent drug remaining at time t_{last} and 'k' is the rate constant for metabolism.

Gastrointestinal Stability. Simulated gastrointestinal fluids were prepared according to USP specifications. Simulated gastric fluid (SGF) was prepared by dissolving 234 mg of NaCl and 37.2 mg of KCl in 100 mL triple distilled water and pH was adjusted to 1.2 with concentrated HCl. Simulated intestinal fluid (SIF) was prepared by dissolving 680 mg of KH_2PO_4 and 90 mg of NaOH in 100 mL triple distilled water and pH was adjusted to 6.8 with orthophosphoric acid. Compounds **6d** and **6j** (5 μg/mL) were incubated in SGF (simulated gastric fluid, pH 1.2) and SIF (simulated intestinal fluid, pH 6.8) for 120 min in a thermostatic oscillating water bath (37 °C and 90 rpm). Samples (100 μL) were taken at different time intervals (0, 15, 30, 45, 60, 90, and 120 min) and were analyzed using HPLC. Stability results were expressed in % remaining vs

time graph. Calculation for stability study data was performed as % parent remaining at different time points relative to the parent at 0 minutes (100% parent).

Animals and Legal Prerequisite. Young, adult male Swiss mice, weighing 20 ± 2 g, were procured from the National Laboratory Animal Center, CSIR-CDRI (Lucknow, India). Mice were housed in well ventilated cages at room temperature (24 ± 2°C) and 40-60 % relative humidity while on a regular 12 h light-dark cycle. The animals were acclimatized for a minimum period of 3 days prior to the experiment. Approval from the Local Animal Ethics Committee was sought and the study protocols were approved before the commencement of the studies.

***In Vivo* Pharmacokinetic Parameters.** Male *Swiss mice* (n = 4) were fasted overnight (12-14 h) before dosing and had free access to water throughout the experimental period. Compound **6j** was administered orally at a dose of 50 mg/kg in 0.25% CMC suspension. Animals were provided with standard diet 3 h after dosing. The mice were anesthetized using ether and blood samples were collected from the retro-orbital plexus into heparinized microfuge tubes at 0.25, 0.50, 1, 2, 3, 5, 7, 9, 24, and 30 h post-dosing. Plasma was harvested by centrifuging the blood at 13000 rpm for 10 min on Sigma 1-15K (Frankfurt, Germany) and stored frozen at –70 ± 10°C until bioanalysis. Each plasma sample (100 μL) was processed using protein precipitation method using acetonitrile containing medicarpin as internal standard (I.S.) 200 μL as protein precipitant, and 10 μL of the supernatant was submitted for LC-MS/MS to get the plasma concentration-time profile of **6j**.

ASSOCIATED CONTENT

Supporting Information

Spectra for ^{1}H, ^{13}C, and HRMS of all compounds are available free of charge via the internet at http://pubs.acs.org.

AUTHOR INFORMATION

Corresponding Authors

*P.P.Y.: phone: +91-522-2772450, Ext. 4761/4762; Fax: +91-522-2771942/2771970; Email: pp_yadav@cdri.res.in

*S.K.: phone: +91-522-2772450, Ext. 4495; Email: susantakar@cdri.res.in

Author Contributions

#D.A. and P.K.Y. contributed equally to this work.

ACKNOWLEDGMENTS

D.A., P.K.Y., R.K.M., K.S.R.R., and P.V. are thankful to CSIR, New Delhi and O.P.S.P. and N.P. are thankful to UGC, New Delhi, India for financial assistance. The authors are thankful Mr. Anoop K. Srivastava for technical support and SAIF-CDRI, Lucknow, India for providing spectral and analytical data. The authors also acknowledge Dr. M. I. Siddiqi for providing access to computational resources. This work was supported by CSIR network project "HOPE" (BSC0114) and Department of Science and Technology, India. The transgenic *L. donovani* promastigotes were originally procured from Dr. Neena Goyal, Division of Biochemistry, CSIR-CDRI, Lucknow, India. CSIR-CDRI communication no. is 9406.

ABBREVIATIONS USED

MCRs, Multicomponent reactions; VL, visceral leishmaniasis; iNOS, inducible nitric oxide synthase; SAR, structure-activity relationship; ip, intraperitoneally; IC_{50}, half maximal inhibitory concentration; CC_{50}, 50% reduction of cell viability of treated culture cells with respect to untreated culture; MIC, maximum inhibitory concentration; SI, selectivity index; MMP, mitochondrial membrane potential; NO, nitric oxide; PI, propidium iodide; FITC, fluorescein isothiocyanate; TUNEL, Terminal deoxynucleotidyl transferase dUTP nick end labelling; SGF,

simulated gastric fluid; SIF, simulated intestinal fluid; FBS, fetal bovine serum; AUC, area under the curve; $t_{1/2}$, half-time; C_{max}, maximum concentration; HPLC, high-performance liquid chromatography; HRMS, high-resolution mass spectrometry; NMR, nuclear magnetic resonance; IR, infrared spectroscopy; TLC, thin-layer chromatography; DMSO, dimethyl sulfoxide; CH_3CN, acetonitrile; EtOH, ethanol; CH_3COOH, acetic acid;

REFERENCES

1. (a) Nagle, A. S.; Khare, S.; Kumar, A. B.; Supek, F.; Buchynskyy, A.; Mathison, C. J. N.; Chennamaneni, N. K.; Pendem, N.; Buckner, F. S.; Gelb, M. H.; Molteni, V. Recent developments in drug discovery for leishmaniasis and human African trypanosomiasis. *Chem. Rev.*, **2014**, *114*, 11305–11347. (b) Renslo, A. R.; McKerrow, J. H. Drug discovery and development for neglected parasitic diseases. *Nat. Chem. Biol.* **2006**, *2*, 701-710.
2. Leishmaniasis. Fact sheet No. 375. World Health Organization: Geneva **2014**. Available from: http://www.who.int/mediacentre/factsheets/fs375/en/ (accessed on November 16, 2015).
3. (a) Hussain, H.; Al-Harrasi, A.; Al-Rawahi, A.; Green, I. R.; Gibbons, S. Fruitful decade for antileishmanial compounds from 2002 to late 2011. *Chem. Rev.* **2014**, *114*, 10369-10428. (b) Sangshetti, J. N.; Khan, F. A. K.; Kulkarni, A. A.; Arote, R.; Patil, R. H. Antileishmanial drug discovery: comprehensive review of the last 10 years. *RSC Adv.* **2015**, *5*, 32376-32415.
4. Sundar, S.; More, D. K.; Singh, M. K.; Singh, V. P.; Sharma, S.; Makharia, A. Failure of pentavalent antimony in visceral leishmaniasis in India: report from center of the indian epidemic. *Clin. Infect. Dis.* **2000**, *31*, 1104-1107.
5. (a) Freitas-Junior, L. H.; Chatelin, E.; Kim, H. A.; Siqueira-Neto, J. L. Visceral leishmaniasis treatment: What do we have, what do we need and how to deliver it? *Int. J.*

Parasitol: Drugs Drug Resist. **2012**, *2*, 11-19. (b) Dorlo, T. P. C.; Van Thiel, P. A. M.; Huitema, A. D. R.; Keizer, R. J.; De Vries, H. J. C.; Beijnen, J. H.; De Vries, P. J. Pharmacokinetics of miltefosine in old world cutaneous leishmaniasis patients. *Antimicrob. Agents Chemother.* **2008**, *52*, 2855-2860. (c) Jha, T. K. Drug unresponsiveness and combination therapy for kala-azar. *Indian J. Med. Res.* **2006**, *123*, 389-398.

6. Bogdan, C.; Gessner, A.; Solbach, W.; Rollinghoff, M. Invasion, control and persistence of *Leishmania* parasites. *Curr. Opin. Immunol.* **1996**, *8*, 517-525.
7. Olivier, M.; Gregory, D. J.; Forget, G. Subversion mechanisms by which *Leishmania* parasites can escape the host immune response: a signaling point of view. *Clin. Microbiol. Rev.* **2005**, *18*, 293-305.
8. Assreuy, J.; Cunha, F. Q.; Epperlein, M .; Noronha-Dutra, A.; O'Donnell, C. A.; Liew, F. Y.; Moncada, S. Production of nitric oxide and superoxide by activated macrophages and killing of *Leishmania major. Eur. J. Immunol.* **1994**, 2*4*, 672-676.
9. Vitaku, E.; Smith, D. T.; Njardarson, J. T. Analysis of the structural diversity, substitution patterns, and frequency of nitrogen heterocycles among U.S. FDA approved pharmaceuticals. *J. Med. Chem.* **2014**, *57*, 10257-10274.
10. Roy, A.; Das, B. B.; Ganguly, A.; Dasgupta, S. B.; Khalkho, N. V. M.; Pal, C.; Dey, S.; Giri, V. S.; Jaisankar, P.; Dey, S.; Majumder, H. K. An insight into the mechanism of inhibition of unusual bi-subunit topoisomerase I from *Leishmania donovani* by 3,3′-di-indolylmethane, a novel DNA topoisomerase I poison with a strong binding affinity to the enzyme. *Biochem. J.* **2008**, *409*, 611-622.

11. Agarwal, A.; Ramesh, Ashutosh, Goyal, N.; Chauhan, P. M. S.; Gupta, S. Dihydropyrido[2,3-d]pyrimidines as a new class of antileishmanial agents. *Bioorg. Med. Chem.* **2005**, *13*, 6678-6684.

12. Mello, H. d.; Echevarria, A.; Bernadino, A. M.; Canto-Cavalheiro, M.; Leon, L. L. Antileishmanial pyrazolopyridine derivatives: Synthesis and structure-activity relationship analysis. *J. Med. Chem.* **2004**, *47*, 5427-5432.

13. Reichwald, C.; Shimony, O.; Dunkel, U.; Sacerdoti-Sierra, N.; Jaffe, C. L.; Kunick, C. 2-(3-Aryl-3-oxopropen-1-yl)-9-tert-butyl-paullones: A new antileishmanial chemotype. *J. Med. Chem.* **2008**, *51*, 659-665.

14. Porwal, S.; Chauhan, S. S.; Chauhan, P. M. S.; Shakya, N.; Verma, A.; Gupta, S. Discovery of novel antileishmanial agents in an attempt to synthesize pentamidine-aplysinopsin hybrid molecule. *J. Med. Chem.* **2009**, *52*, 5793-5802.

15. (a) Mowbray, C. E.; Braillard, S.; Speed, W.; Glossop, P. A.; Whitlock, G. A.; Gibson, K. R.; Mills, J. E. J.; Brown, A. D.; Gardner, J. M. F.; Cao, Y.; Hua, W.; Morgans, G. L.; Feijens, P-B.; Matheeussen, A.; Maes, L. J. Novel amino-pyrazole ureas with potent *in vitro* and *in vivo* antileishmanial activity. *J. Med. Chem.* **2015**, *58*, 9615-9624. (b) Horn, K. S. V.; Zhu, X.; Pandharkar, T.; Yang, S.; Vesely, B.; Vanaerschot, M.; Dujardin, J.-C.; Rijal, S.; Kyle, D. E.; Wang, M. Z.; Werbovetz, K. A.; Manetsch, R. Antileishmanial activity of a series of N^2,N^4-disubstituted quinazoline-2,4-diamines. *J. Med. Chem.* **2014**, *57*, 5141-5156.

16. (a) Rotstein, B. H.; Zaretsky, S.; Rai, V.; Yudin, A. K. Small heterocycles in multicomponent reactions. *Chem. Rev.* **2014**, *114*, 8323-8359. (b) Shiri, M. Indoles in multicomponent processes (MCPs). *Chem. Rev.* **2012**, *112*, 3508-3549. (c) Domling, A.; Wang, W.; Wang, K. Chemistry and biology of multicomponent reactions. *Chem. Rev.* **2012**,

112, 3083-3135. (d) Graaff, C. d.; Ruijter, E.; Orru, R. V. A. Recent developments in asymmetric multicomponent reactions. *Chem. Soc. Rev.* **2012**, *41*, 3969-4009.

17. (a) Tu, S.; Wang, Q.; Zhang, Y.; Xu, J.; Zhang, J.; Zhu, X.; Shi, F. Design and synthesis of new and significative bifunctional compounds containing two pyrazolo[3,4-*b*]pyridine nucleus through multicomponent reaction under microwave irradiation. *J. Heterocycl. Chem.* **2007**, *44*, 811-814. (b) Chen, H.; Shi, D. Efficient one-pot synthesis of novel spiro-oxindole derivatives via three-component reaction in aqueous medium. *J. Comb. Chem.* **2010**, *12*, 571-576. (c) Karnakar, K.; Murthy, S. N.; Ramesh, K.; Satish, G.; Nanubolu, J. B.; Nageswar, Y. V. D. Polyethylene glycol (PEG-400): an efficient and recyclable reaction medium for the synthesis of pyrazole[3,4-*b*]quinolone derivatives. *Tetrahedron Lett.* **2012**, *53*, 2897-2903. (d) Hao, Y.; Xu, X-P.; Chen, T.; Zhao, L-L.; Ji, S-J. Multicomponent approaches to 8-carboxylnaphthyl-functionalized pyrazole[3,4-*b*]pyridine derivatives. *Org. Biomol. Chem.* **2012**, *10*, 724-728. (e) Chebanov, V. A.; Saraev, V. E.; Desenko, S. M.; Chernenko, V. N.; shishkina, S. V.; shishkin, O. V.; Kobzar, K. M.; Kappe, C. O. One-pot, multicomponent route to pyrazoloquinolizinones. *Org. Lett.* **2007**, *9*, 1691-1694. (f) Jacominia, A. P.; Silvaa, M. J. V.; Silvaa, R. G. M.; Gonçalvesa, D. S.; Volpatob, H.; Bassoa, E. A.; Paulac, F. R.; Nakamurab, C. V.; Sarragiottoa, M. H.; Rosa, F. A. Synthesis and evaluation against Leishmania amazonensis of novel pyrazolo[3,4-*d*]pyridazinone-N-acylhydrazone-(bi)thiophene hybrids. *Eur. J. Med. Chem.* **2016**, *124*, 340-349.

18. Slatt, J.; Romero, I.; Bergman, J. Cyanoacetylation of indoles, pyrroles and aromatic amines with the combination cyanoacetic acid and acetic anhydride. S*ynthesis* **2004**, 1*6*, 2760-2765.

19. Ahmad, I.; Mishra, N. K.; Ghosh, T. 5-(1H-Indol-3-yl)-pyrazolyl derivatives as colorimetric sensor for anions. *J. Inclusion Phenom. Macrocyclic Chem.* **2013**, *76*, 183-191.

20. Toton, E.; Ignatowicz, E.; Bernard, M. K.; Kujawski, J.; Rybczynska, M. Evaluation of apoptotic activity of new condensed pyrazole derivatives. *J. Physiol. Pharmacol.* **2013,** *64,* 115-123.

21. Reimao, J. Q.; Miguel, D. C.; Taniwaki, N. N.; Trinconi, C. T.; Yokoyama-Yasunaka, J. K.; Uliana, S. R. Antileishmanial activity of the estrogen receptor modulator raloxifene. *PLoS Neglected Trop. Dis.* **2014,** *8*, e2842.

22. Baell, J. B.; Holloway, G. A. New substructure filters for removal of pan assay interference compounds (PAINS) from screening libraries and for their exclusion in bioassays. *J. Med. Chem.* **2010**, *53*, 2719-2740.

23. Ashutosh; Gupta, S.; Ramesh; Sundar, S.; Goyal, N. Use of *Leishmania donovani* field isolates expressing the luciferase reporter gene in *in vitro* drug screening. *Antimicrob Agents Chemother.* **2005**, *49*, 3776-3783.

24. Mosmann, T. Rapid colorimetric assay for cellular growth and survival: Application to proliferation and cytotoxicity assays. *J. Immunol. Methods* **1983**, *65*, 55-63.

25. Huber, W.; Koella, J. C. A comparison of three methods of estimating EC_{50} in studies of drug resistance of malaria parasites. *Acta Trop*. **1993**, *55*, 257-261.

26. Shivahare, R.; Vishwakarma, P.; Parmar, N.; Yadav, P. K.; Haq, W.; Srivastava, M.; Gupta, S.; Kar, S. Combination of liposomal CpG oligodeoxynucleotide 2006 and miltefosine induces strong cell-mediated immunity during experimental visceral leishmaniasis. *PLoS One* **2014**, 9, e94596.

Table of Contents Graphic

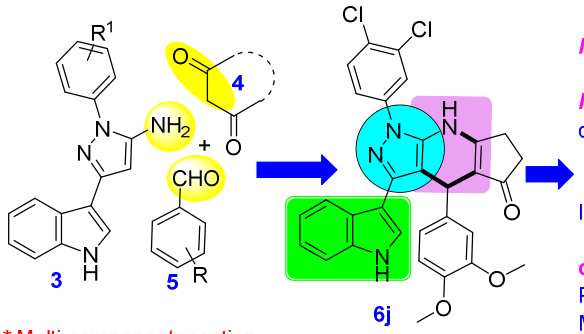

* Multi-component reaction
* No column chromatography for most of the compounds

***In vitro*:** IC_{50} = 4.05 µM against amastigote
CC_{50} = 438.5 µM; SI = 108.2

***In vivo*:** >90% inhibition of spleen and liver parasite burden in L. donovani/mice model

Combination therapy in sub-curative doses

6j (25 mg/kg) + Miltefosine (5 mg/kg) = >89% and >96% inhibition in liver and spleen parasite burden

Effects of compound 6j

on leishmania parasite:	Host response:
Phosphatidyl serine externalisation	IL-12, TNF-α, Nitric oxide ↑
MMP loss, DNA fragmentation	IL-10, TGF-β ↓
Apoptosis	